

# Lipid A in outer membrane vesicles shields bacteria from polymyxins

Marie Burt<sup>1</sup> | Georgia Angelidou<sup>2,3</sup> | Christopher Nils Mais<sup>4</sup> | Christian Preußner<sup>5,6</sup> |  
Timo Glatter<sup>3</sup> | Thomas Heimerl<sup>4</sup> | Rüdiger Groß<sup>7</sup> | Javier Serrania<sup>4</sup> |  
Gowtham Boosarpu<sup>1</sup> | Elke Pogge von Strandmann<sup>5,6</sup> | Janis A. Müller<sup>8</sup>  | Gert Bange<sup>4</sup> |  
Anke Becker<sup>4</sup> | Mareike Lehmann<sup>1,9,10</sup> | Danny Jonigk<sup>11,12</sup> | Lavinia Neubert<sup>11,13</sup> |  
Hinrich Freitag<sup>11,13</sup> | Nicole Paczia<sup>2</sup> | Bernd Schmeck<sup>1,4,10,14,15,16</sup> | Anna Lena Jung<sup>1,16</sup> 

<sup>1</sup>Institute for Lung Research, Universities of Giessen and Marburg Lung Center, German Center for Lung Research (DZL), Philipps-University Marburg, Marburg, Germany

<sup>2</sup>Core Facility for Metabolomics and Small Molecules Mass Spectrometry, Max Planck Institute for Terrestrial Microbiology, Marburg, Germany

<sup>3</sup>Core Facility for Mass Spectrometry and Proteomics, Max Planck Institute for terrestrial Microbiology, Marburg, Germany

<sup>4</sup>Center for Synthetic Microbiology (SYNMIKRO), Philipps-University Marburg, Marburg, Germany

<sup>5</sup>Institute for Tumor Immunology, Philipps-University Marburg, Marburg, Germany

<sup>6</sup>Core Facility - Extracellular Vesicles, Philipps-University Marburg, Marburg, Germany

<sup>7</sup>Institute of Molecular Virology, Ulm University Medical Center, Ulm, Germany

<sup>8</sup>Institute of Virology, Philipps-University Marburg, Marburg, Germany

<sup>9</sup>Comprehensive Pneumology Center (CPC), Institute of Lung Health and Immunity, Helmholtz Zentrum München, German Center for Lung Research (DZL), Munich, Germany

<sup>10</sup>Institute for Lung Health (ILH), Giessen, Germany

<sup>11</sup>Biomedical Research in Endstage and Obstructive Lung Disease Hannover (BREATH), German Center of Lung Research (DZL), Hannover, Germany

<sup>12</sup>Institute of Pathology, University Medical Center RWTH University of Aachen, Aachen, Germany

<sup>13</sup>Institute of Pathology, Hannover Medical School, Hannover, Germany

<sup>14</sup>Department of Medicine, Pulmonary and Critical Care Medicine, University Medical Center Marburg, Universities of Giessen and Marburg Lung Center, Philipps-University Marburg, Marburg, Germany

<sup>15</sup>Member of the German Center for Infectious Disease Research (DZIF), Marburg, Germany

<sup>16</sup>Core Facility Flow Cytometry – Bacterial Vesicles, Philipps-University Marburg, Marburg, Germany

## Correspondence

Anna Lena Jung, Institute for Lung Research, Universities of Giessen and Marburg Lung Center, German Center for Lung Research (DZL), Philipps-University Marburg, Marburg, 35043, Germany.  
Email: [anna.jung@uni-marburg.de](mailto:anna.jung@uni-marburg.de)

## Funding information

Hessisches Ministerium für Wissenschaft und Kunst, Grant/Award Number: LOEWE/2/13/519/03/06.001(0002)/74; Deutsche Forschungsgemeinschaft, Grant/Award Numbers: 512453064, SFB/TR-84 TP C01; von

## Abstract

The continuous emergence of multidrug-resistant bacterial pathogens poses a major global healthcare challenge, with *Klebsiella pneumoniae* being a prominent threat. We conducted a comprehensive study on *K. pneumoniae*'s antibiotic resistance mechanisms, focusing on outer membrane vesicles (OMVs) and polymyxin, a last-resort antibiotic. Our research demonstrates that OMVs protect bacteria from polymyxins. OMVs derived from Polymyxin B (PB)-stressed *K. pneumoniae* exhibited heightened protective efficacy due to increased vesiculation, compared to OMVs from unstressed *Klebsiella*. OMVs also shield bacteria from different bacterial families. This was validated ex vivo and in vivo using precision cut lung slices (PCLS) and *Galleria mellonella*. In all models, OMVs protected *K. pneumoniae* from PB and reduced the

This is an open access article under the terms of the [Creative Commons Attribution-NonCommercial-NoDerivs License](https://creativecommons.org/licenses/by-nc-nd/4.0/), which permits use and distribution in any medium, provided the original work is properly cited, the use is non-commercial and no modifications or adaptations are made.

© 2024 The Author(s). *Journal of Extracellular Vesicles* published by Wiley Periodicals LLC on behalf of International Society for Extracellular Vesicles.

Behring-Röntgen-Stiftung, Grant/Award Numbers: 66-LV07, 71\_0002; German Center for Lung Research (DZL); German Ministry for Education and Research (BMBF), Grant/Award Numbers: ERACo-SysMed2 SysMed-COPD-FKZ 03IL0140, JPIAMR Pneumo-AMRProtect-FKZ 01KI702, e:Med CAPSYS-FKZ 01X1304E/01ZX1304F

associated stress response on protein level. We observed significant changes in the lipid composition of OMVs upon PB treatment, affecting their binding capacity to PB. The altered binding capacity of single OMVs from PB stressed *K. pneumoniae* could be linked to a reduction in the lipid A amount of their released vesicles. Although the amount of lipid A per vesicle is reduced, the overall increase in the number of vesicles results in an increased protection because the sum of lipid A and therefore PB binding sites have increased. This unravels the mechanism of the altered PB protective efficacy of OMVs from PB stressed *K. pneumoniae* compared to control OMVs. The lipid A-dependent protective effect against PB was confirmed in vitro using artificial vesicles. Moreover, artificial vesicles successfully protected *Klebsiella* from PB ex vivo and in vivo. The findings indicate that OMVs act as protective shields for bacteria by binding to polymyxins, effectively serving as decoys and preventing antibiotic interaction with the cell surface. Our findings provide valuable insights into the mechanisms underlying antibiotic cross-protection and offer potential avenues for the development of novel therapeutic interventions to address the escalating threat of multidrug-resistant bacterial infections.

#### KEYWORDS

antimicrobial peptides (AMP), bacterial extracellular vesicles, bacterial resistance mechanisms, last-resort antibiotic, lipid A, multi-drug resistance (MDR), polymyxins

## 1 | INTRODUCTION

*Klebsiella pneumoniae* (*K. pneumoniae*; *Kp*) is a gram-negative opportunistic pathogen well-known for causing severe invasive infection outcomes, like pneumonia and bloodstream infections (Li & Huang, 2017), as well as chronic inflammatory airway diseases as cystic fibrosis and bronchiectasis (Hamdi et al., 2016; Rafiee et al., 2017). It possesses a multitude of virulence factors and exhibits the ability to colonize human mucosal surfaces, which constitutes a critical step in the progression of infection. The persistence and ability of *K. pneumoniae* to survive within the host pose significant challenges for effective treatment strategies (Paczosa & Meccas, 2016).

In recent years, the clinical impact of *K. pneumoniae* infections has been exacerbated by the emergence of hypervirulent strains (Russo & Marr, 2019) and multidrug-resistant (MDR) variants (Bassetti et al., 2018). These strains display enhanced virulence traits, such as increased capsular polysaccharide production (Cheng et al., 2010; Liu et al., 2017), hypermucoviscosity (Fang et al., 2004), and improved adhesion to host cells (Riwu et al., 2022; Schroll et al., 2010). Simultaneously, MDR *K. pneumoniae* strains have developed resistance mechanisms against multiple classes of antibiotics, severely limiting treatment options. The alarming rise in MDR *Klebsiella* infections prompted the World Health Organization to classify *Klebsiella* as a high-priority antibiotic-resistant pathogen (World Health Organization, 2017), necessitating immediate action to unravel pathogenicity mechanisms and to identify potential therapeutic targets. In the clinical management of *K. pneumoniae* infections, a range of antibiotics is typically employed, including Carbapenems, Cephalosporins, Fluoroquinolones, and Aminoglycosides (Bush & Vazquez-Pertejo, 2022; Robert Koch-Institut (RKI) 2012). However, the rise of MDR *K. pneumoniae* strains has rendered many of these antibiotics ineffective, necessitating the use of last-resort antibiotics. Though, even Tigecycline, Ceftazidime-Avibactam and polymyxins (Michalopoulos & Falagas, 2008) are being challenged due to emerging resistances (Ayoub Moubareck, 2020), highlighting the critical need for novel treatment strategies.

Polymyxins, including Polymyxin B (PB) and Colistin, are antimicrobial peptides, used as cationic polypeptide antibiotics primarily targeting gram-negative bacteria, applied as a measure of last resort topically in the airways or systemically (Li et al., 2005). Polymyxins disrupt the bacterial outer membrane by displacing divalent cations and binding to lipopolysaccharide (LPS) molecules, particularly lipid A, leading to membrane disintegration, permeabilization, and bacterial cell death (Ayoub Moubareck, 2020; Michalopoulos & Falagas, 2008). Even though polymyxins can cause nephrotoxicity and neurotoxicity and have therefore not been used for a long time, interest in them has increased over the last two decades due to the rise of MDR bacteria and the lack of new antibiotics (Tran et al., 2016).

Outer membrane vesicles (OMVs) are nano-sized structures derived from the outer membrane of gram-negative bacteria (Mashburn & Whiteley, 2005), involved in intercellular communication (Caruana & Walper, 2020; Mashburn & Whiteley, 2005) and immune response modulation (Bierwagen et al., 2023; Jung et al., 2016, 2017). They also contribute to protection against surface-attacking agents, as shown for bacteriophages and the antibiotic Melittin (Kulkarni et al., 2015; Manning & Kuehn, 2011). OMVs act as crucial vehicles for transporting cargo molecules, including proteins, lipids, nucleic acids and virulence factors

(Kulp & Kuehn, 2010). The quantity, composition and cargo of OMVs can be influenced by environmental conditions, stressors, and the physiological state of the cells (Macdonald & Kuehn, 2013; Maestre-Carballa et al., 2019; McMillan und Kuehn, 2023; Zavan et al., 2023; Zingl et al., 2020). OMVs enable bacteria to interact with their surroundings and neighbouring cells (Zhao et al., 2022), for example by facilitating the dissemination of virulence factors (Ellis & Kuehn, 2010; Olaya-Abril et al., 2014). Furthermore, proteomic analyses have revealed that OMVs carry a wide range of cargo, including proteins derived from the periplasmic space, outer and inner membrane and cytoplasm (Bhar et al., 2021; Liu et al., 2019). Distinct compositions have been observed between *K. pneumoniae* OMVs and their source membrane, suggesting a selective sorting mechanism potentially involving the polysaccharide groups of LPS (Cahill et al., 2015). Moreover, OMVs have been implicated in antibiotic resistance (Zhang et al., 2023), by facilitating horizontal gene transfer (Johnston et al., 2023) fostering the emergence of antibiotic resistance in gram-negative bacteria (Caruana & Walper, 2020; Dell'Annunziata et al., 2021; Dhital et al., 2022; Kim et al., 2020). OMVs shield bacteria from the impacts of antibiotics through various mechanisms, employing antibiotic-degrading enzymes like  $\beta$ -lactamases and aminoglycoside-inactivating enzymes, or capturing membrane-active antibiotics like Melittin and PB by binding it (Ciofu et al., 2000; Kulkarni et al., 2015). Additionally, treatment of susceptible *Klebsiella* strains with PB can alter the lipid composition of their OMVs (Jasim et al., 2018), potentially acting as a shield against antibiotic attacks. To date, the exact mechanism and importance of different membrane components by which OMVs capture and bind PB has not been elucidated. Moreover, the impact of OMVs derived from PB-stressed *K. pneumoniae* on antibiotic resistance is yet not known. Given that PB is used as an antibiotic of last resort for MDR bacteria, like *K. pneumoniae*, this highlights the critical need for further investigation to understand how OMVs contribute to antibiotic protection.

Here, we investigated the impact of OMVs from PB-stressed *K. pneumoniae* in contrast to control *K. pneumoniae* on bacterial protection against the last-line antibiotic class polymyxins. In this study, we found that OMVs protect various bacteria from polymyxins in vitro, ex vivo and in vivo. Furthermore, we showed that OMVs from PB-stressed *K. pneumoniae* exhibited an increased protective effect against PB by increased vesiculation upon PB treatment. We demonstrated that OMVs bind polymyxins, thereby acting as a decoy to prevent the binding of polymyxins to the bacterial membrane.

## 2 | MATERIAL AND METHODS

### 2.1 | Chemicals

LB media, MacConkey agar, Colistin sulfate and sodium acetate were acquired from Carl Roth GmbH & Co. KG (Karlsruhe, Germany). PBS was obtained from Capricorn Scientific GmbH (Ebsdorfergrund, Germany). Ham's F12 medium was purchased from GE Healthcare Europe (Freiburg, Germany). Polymyxin B was supplied by Merck Millipore (Billerica, USA). Gentamicin was obtained from Gibco Life Technologies (Carlsbad, USA) and Meropenem from Cayman Chemicals (Ann Arbor, USA). Methanol was acquired from Merck KGaA (Darmstadt, Germany). Chloroform was purchased from Acros Organics (Geel, Belgium). LPS (*Salmonella minnesota* R595, TLR grade) was supplied by Enzo Life Sciences (Lausen, Austria). All lipids were obtained from Avanti® Polar Lipids Inc. (Birmingham, USA). All other applied chemicals were of analytical grade and acquired from commercial sources.

### 2.2 | Bacterial culture and isolation of outer membrane vesicles

*Klebsiella pneumoniae* (*K. pneumoniae*, Kp; #700721/MGH78578), *Salmonella enterica* serovar Typhimurium (*Sal*; #14028) and *Escherichia coli* (*Ec*, #25922) were obtained from American Type Culture Collection (Rockville, MD, USA). A wildtype *Legionella pneumophila* strain Corby and a clinical isolate of *K. pneumoniae* (Kp-i) were used. *Pseudomonas aeruginosa* were kindly provided by PD Dr. med. univ. Ulrich Matt. For outer membrane vesicle (OMV) isolation bacteria were streak plated on MacConkey agar plates and grown overnight (37°C). Bacteria were used to inoculate 1 L of LB media and were incubated under continuous shaking until the late logarithmic phase (37°C, 160 rpm, MaxQ 6000, Thermo Fisher Scientific, Karlsruhe, Germany). To generate vesicles from stressed bacteria, sub-inhibitory concentrations of Polymyxin B (PB OMVs) or Gentamicin (genta OMVs) were added at the beginning of the shaking liquid culture. When bacteria reached the late logarithmic phase, samples were serially diluted, streaked on agar plates and incubated at 37°C overnight to check for contamination. Cultures were centrifuged three times (4500 × g, 4°C, 20 min; Multifuge X3R, Thermo Fisher Scientific) to remove bacterial cells and to obtain the supernatant. Afterwards, the supernatant was sterile filtered (0.22 µm filter; Sarstedt, Nümbrecht, Germany), stored over night at 4°C and concentrated via ultra-filtration using 100 kDa molecular weight cut-off filters (Merck KGaA). To check for possible contamination, 5 µL of the concentrate were plated on blood agar plates (BD, New Jersey, USA) and incubated overnight at 37°C. The sterile concentrate was stored at -20°C and used to purify vesicles either by size-exclusion chromatography (SEC) or by ultracentrifugation. For SEC, qEVOoriginal/ 70 nm Gen 1 columns (IZON Science LTD, Lyon, France) were pre-washed with 10 mL 0.1 µm filtered PBS (Cytiva, Marlborough, USA) according to the manufacturer's protocol and 500 µL concentrate was loaded. Vesicles

were eluted with 0.1  $\mu\text{m}$  filtered PBS in fractions 7–12 (500  $\mu\text{L}$ /fraction). The presence of bacterial extracellular vesicles (EVs) was determined by nano-flow cytometry (nFCM; NanoFCM Co., Ltd, Nottingham, UK). The vesicle-containing fractions were pooled and concentrated using 100 kDa molecular weight cut-off filters (Merck KGaA) to 200–400  $\mu\text{L}$ . The vesicle concentration was determined by nano-flow cytometry (nFCM) as described below. For ultracentrifugation, the concentrated supernatant was spun at  $100,000 \times g$ , 3 h, 4°C (ultracentrifuge type Sorvall discovery™ 90 SE: Hitachi, Chiyoda, Japan; rotor type 70Ti: Beckman Coulter, Brea, USA). The pellet was washed with sterile, 0.1  $\mu\text{m}$  filtered PBS and again ultracentrifuged ( $100,000 \times g$ , 3 h, 4°C). Afterwards, pellets were resuspended in sterile, 0.1  $\mu\text{m}$  filtered PBS and protein content was determined by Pierce BCA protein assay kit according to the manufacturer's instructions (Thermo Fisher Scientific). For experiments, equal amounts of OMV-associated proteins or equal numbers of vesicles were used. After both purification methods, OMVs were checked for bacterial contamination by plating them on blood agar plates. Isolated OMVs were stored at  $-80^\circ\text{C}$  in small aliquots to minimize repeated freeze-thaw cycles.

### 2.3 | Transmission electron microscopy

Transmission electron microscopy was performed as recently described (Bierwagen et al., 2023).

### 2.4 | nFCM

For the nano-flow cytometry, a NanoAnalyzer (NanoFCM Co., Ltd, Nottingham, UK) equipped with a 488 nm and a 638 nm laser was calibrated using 200 nm polystyrene beads (NanoFCM Co.) with a defined concentration of  $2.08 \times 10^8$  particles/mL, which were also used as a reference for the particle concentration. Additionally, monodisperse silica beads (NanoFCM Co., Ltd, Nottingham, UK) of four different diameters (68; 91; 113; 155 nm) were used as size reference standards. As background, freshly filtered (0.1  $\mu\text{m}$ )  $1 \times$  TE buffer pH7.4 (Lonza, Basel, Switzerland) was used and subtracted from all other measurements. Data was collected for 1 min with a sample pressure of 1.0 kPa and particle concentration and size distribution were calculated using NanoFCM software (NF Profession V2.0).

### 2.5 | Polymyxin B-resistant *K. pneumoniae*

To generate a Polymyxin B resistant *K. pneumoniae* (KpR) strain, the PB sensitive *K. pneumoniae* strain ATCC #700721 was used. *Klebsiella* were streak plated on MacConkey agar plates and grown overnight at 37°C. A single colony was used to inoculate 2 mL LB medium with 1  $\mu\text{g}/\text{mL}$  PB for overnight culture (37°C, 160 rpm). Each day, 100  $\mu\text{L}$  of the overnight culture was used to inoculate 2 mL of fresh LB medium, doubling PB, until a concentration of 64  $\mu\text{g}/\text{mL}$  PB was reached. KpR were frozen in 20% glycerol (Carl Roth GmbH & Co. KG), stored at  $-80^\circ\text{C}$  and thawed when needed.

### 2.6 | Sequencing of KpR

Total DNA for resequencing was purified using a DNeasy Blood and Tissue kit (Qiagen, Hilden, Germany). DNA libraries for sequencing were generated by applying a Nextera XT DNA Library Preparation kit (Illumina, San Diego, USA), and sequencing was performed on a MiSeq Desktop Sequencer (Illumina) using a MiSeq Reagent kit, version 3, for 275  $\times$  bp paired-end reads (Illumina). At least 2.5 million reads were obtained for each sample. The investigation for single nucleotide variants was carried out using the Basic Variant Detection tool (Qiagen, v.2.3) of CLC Genomic Workbench (Qiagen, v.22.0.2) with a minimum coverage of 10, minimum count of eight and minimum frequency of 80% for mapped reads.

### 2.7 | Bacterial viability assay

*K. pneumoniae* were streak plated on MacConkey agar plates and grown overnight at 37°C. A single colony was used to inoculate 2 mL LB media for overnight culture (37°C, 160 rpm). Bacterial culture was transferred to 10 mL fresh LB media and incubated until it reached an OD of 2 (1 h, 37°C, 160 rpm). Total of 2 mL bacterial culture was added to 8 mL fresh LB media and treated with increasing amounts of PB or left untreated for control. Samples were incubated for 90 min (37°C, 160 rpm). As positive control for cell death, bacteria were heat killed (HK; 10 min, 95°C). Samples were washed and stained with propidium iodide using LIVE/DEAD™ BacLight™ Bacterial Viability Kit (Invitrogen by Thermo Fisher Scientific, Waltham, USA) according to the manufacturer's protocol and measured (excitation wavelength: 490 nm, emission wavelength: 635 nm) in technical duplicates in

a black 96-well plate using a microplate reader (infinite F200Pro, Tecan, Männedorf, Switzerland). Results are shown compared to positive control which was set as 100% dead bacteria.

## 2.8 | Outer membrane vesicle release of *K. pneumoniae* under stress conditions

*K. pneumoniae* were grown on MacConkey agar plates overnight (37°C). A single colony of *K. pneumoniae* was used for inoculation of 2 mL LB media for overnight culture, which was then transferred to 10 mL fresh LB media and further incubated (1 h, 37°C, 160 rpm, MaxQ 6000, Thermo Fisher Scientific, Waltham, USA). Equal numbers of bacteria were used for inoculation of fresh LB media with pH 5, pH 9, in NaCl (100 mM), with 50 µg/mL Gentamicin, 1 µg/mL PB, 0.8 µg/mL Colistin, 0.05 mM H<sub>2</sub>O<sub>2</sub> or in regular LB media (90 min, 37°C, 160 rpm). Moreover, *Klebsiella* were incubated in LB media at 20°C or 40°C or in H<sub>2</sub>O. After the incubation time, serial dilutions of the bacteria were plated on MacConkey agar plates, incubated overnight (37°C) and counted to determine bacterial colony forming units (CFU) and to check for possible contamination. Samples were centrifuged (4500 × g, 10 min, 4°C; Multifuge X3R, Thermo Fisher Scientific), the supernatant was sterile filtered (0.22 µm) and measured by nFCM using a NanoAnalyzer (NanoFCM Co., Ltd, Nottingham, UK) as described above to determine the size and number of released vesicles. The relative vesicle release per live cell was calculated and is presented relative to control *K. pneumoniae* grown in complete LB media at 37°C.

## 2.9 | Bacterial growth kinetics

*K. pneumoniae*, *Kp-i*, *E. coli* and *Salmonella* were grown on MacConkey agar plates, and *P. aeruginosa* was grown on blood agar plates overnight at 37°C and used to inoculate LB-media to an OD<sub>600</sub> of 0.0005 (*K. pneumoniae*, *Kp-i*, *E. coli*, *Salmonella*) or 0.005 (*P. aeruginosa*). *L. pneumophila* was grown on buffered charcoal-yeast extract agar plates for 3 days and was used afterwards to inoculate yeast extract broth medium to an OD of 0.5 as previously described (Jung et al., 2016). Of each bacterial inoculation, 100 µL was used per well for growth kinetic experiments using a 96-well plate. Respective concentrations of PB, Gentamicin, Colistin or Meropenem, 10 µg/mL LPS, 10 µg/mL OMVs (based on the protein concentration) or 1.5 × 10<sup>9</sup> OMVs/well (Proteinase K digested or undigested) or 1 × 10<sup>9</sup> artificial vesicles/well were used. Growth kinetics were determined under continuous shaking at 37°C, and the optical density at 600 nm wavelength (OD<sub>600</sub>) was measured every 30 min using a plate reader. All biological replicates were performed in technical triplicates. To compare growth kinetics, the time [h] to reach the mid-log phase (OD<sub>600</sub> = 0.4) was compared. The highest concentration of PB or Colistin that did not significantly alter bacterial growth compared to untreated control bacteria was used to calculate the fold change of antibiotic protection. The fold change indicates how much more antibiotics the bacteria can tolerate in the presence of the respective OMVs/artificial vesicles.

## 2.10 | RNA preparation, high-capacity reverse transcription (HCRT) and real-time quantitative polymerase chain reaction (qPCR)

Bacterial RNA was extracted by phenol-chloroform extraction as previously described (Jung et al., 2016) and DNA was digested. For that, DNase (Roche Holding AG, Basel, Switzerland) was 1:10 diluted in ultra-pure water. Total of 1 µL of diluted DNase was used for 1 µg RNA and 1× DNase buffer (Roche Holding AG, Basel, Switzerland) was added. Samples were incubated at 37°C, 600 rpm for 20 min using a thermomixer. Three times as much ultra-pure water as the sample was added and mixed with the same volume of PCI (Carl Roth GmbH und Co. KG). Samples were shaken vigorously for 15 s, incubated for 3 min at RT and centrifuged for 15 min at 14,000 × g at 4°C. The upper, aqueous phase is used to extract the RNA as described previously (Jung et al., 2016). RNA concentration was measured using NanoDrop (Thermo Fisher Scientific) and reverse transcribed using the High-Capacity RNA-to-cDNA kit (Thermo Fisher Scientific) according to the manufacturer's instructions. Quantitative real-time PCR was performed using a ViiA7 (Thermo Fisher Scientific) with Luna Universal qPCR Mastermix (New England Biolabs) and specific primer pairs. 2<sup>-ΔΔCT</sup> method (Livak & Schmittgen, 2001) was used and x-fold induction was calculated. Results were normalized to corresponding control samples. The expression of *phoP*, *phoQ* and *pmrK* were measured using the housekeeping gene *rpsL* for *K. pneumoniae*. The used primers are listed below.

*rpsL*: fwd: 5'-AAGCCTTAGGACGCTTCACG-3', rev: 5'-ACCTTCCGGGTGTTTCGTTAC-3'  
*phoP*: fwd: 5'-GATGCCGAAGTGCAGAAAG-3', rev: 5'-GTGATGACGTCCTGTGGGTA-3'  
*phoQ*: fwd: 5'-TTGAGCCGGAATTACACCC-3', rev: 5'-GCACGGAAACTTCCACGAAC-3'  
*pmrK*: fwd: 5'-CGGTAACGGTAAGTCGAGCA-3', rev: 5'-CAGGGTGAGCTGAAGTACGG-3'

## 2.11 | Proteinase K digestion of OMVs, SDS-PAGE and silver staining

*Kp*-ctr OMVs ( $1 \times 10^{11}$ ) were incubated with 50  $\mu\text{g}/\text{mL}$  Proteinase K (AppliChem GmbH, Darmstadt, Germany), 4.8% Triton X-100 (Carl Roth GmbH & Co. KG) and 10% Tween-20 (Carl Roth GmbH & Co. KG) for 2 h at 37°C, 300  $\times g$  using a thermomixer (Eppendorf AG, Hamburg, Germany). Afterwards, proteins were precipitated via NaDOC/TCA precipitation (Arnold & Ulbrich-Hofmann, 1999). For this precipitation, samples were mixed with 1/10 of the starting volume with 1% NaDOC solution and with 1/5 of the starting volume with a 50% TCA solution. Samples were mixed vigorously and centrifuged at 13,000  $\times g$ , 4°C for 15 min. Samples were washed in cold acetone (Carl Roth GmbH und Co. KG), centrifuged, resuspended in 40  $\mu\text{L}$  PBS and 10  $\mu\text{L}$  5 $\times$  Laemmli-buffer with  $\beta$ -mercaptoethanol and incubated at 95°C for 5 min. A 12.5% SDS-PAGE was used to separate the proteins (30 min 80 V, followed by 2 h 120 V). Afterwards, the gel was silver stained. For silver staining, the gel was first fixed for 1 h in a fixing solution (50% ethanol (Carl Roth GmbH & Co. KG), 12 % acetic acid, 0.5 mL/L 37% formaldehyde (Carl Roth GmbH & Co. KG)) and washed two times with 50% ethanol for 20 min and once washed with 30% ethanol for 20 min. Then, the gel was incubated in a pretreatment solution for 1 min and three times washed with ultra-pure water for 20 s. Afterwards, the gel was transferred into silver staining solution (2 g/L  $\text{AgNO}_3$  (Carl Roth GmbH & Co. KG), 750  $\mu\text{L}/\text{L}$  37% formaldehyde (Carl Roth GmbH & Co. KG)) for 20 min and into developing solution as long as needed to see proper bands.

## 2.12 | Preparation of human PCLS (hPCLS)

Human precision cut lung slices (PCLS) were extracted from fibrotic lung explants during lung allograft transplantation and from lung tumour resections derived from patients with primary pulmonary carcinoma and from patients with metastases. The tissue was processed as described previously by Preuß et al. (Preuß et al., 2022). All tissue donors gave informed consent for participating in the study. The study was approved by the local ethics committee of Hannover Medical School (MHH Hannover, Germany, no. 8867\_BO\_K2020 and no. 2923-2014).

## 2.13 | Preparation of mouse PCLS (mPCLS)

Wildtype healthy female C57BL6 aged 31 weeks mice were sacrificed using intramuscular injections of a cocktail consisting of Ketamine, Xylazine and Heparin. The trachea was exposed and intubated, the diaphragm and rib cage were then cut open, and the lungs were flushed through the pulmonary artery by injecting sterile PBS into the right ventricle of the heart to remove blood. Once the lungs appeared white, 2 mL of 3% low temperature gelling agarose (Sigma) dissolved in DMEM-F12 (Life Technologies GmbH, USA) was injected into the lungs through the tracheal cannula using a syringe pump. The lungs were then pulled out of the chest and kept at 4°C in DMEM-F12 until slicing. The lobes were then separated, and precision cut into 300  $\mu\text{m}$  slices using a vibratome (7000-smz2 from Campden Instruments) as described previously in Uhl et al. (2015). Individual slices were then kept in culture individually in 24-well plates in DMEM-F12 supplemented with 0.1% FBS, 1% Penicillin/Streptomycin (Life Technologies GmbH, USA) and 1% Amphotericin B (Life Technologies GmbH, USA).

## 2.14 | *K. pneumoniae* infection of PCLS

One day prior to infection, media was changed to Ham's F12 blank media (without FCS and with 1% Amphotericin B). PCLS were infected with  $1 \times 10^4$  *K. pneumoniae*, and 6  $\mu\text{g}/\text{mL}$  PB and 18  $\mu\text{g}/\text{mL}$  *Kp*-PB OMVs (hPCLS) or  $2.5 \times 10^{10}$  artificial vesicles containing 40% Kdo2-lipid A (KLA) (mPCLS) were added at the same timepoint and incubated at 37°C, 5%  $\text{CO}_2$ . Four (hPCLS and mPCLS) and eight (hPCLS) hours after infection, supernatant of the infected PCLS were used to determine bacterial growth via CFU assay. For that, supernatant was serially diluted, plated on MacConkey agar plates and incubated overnight (37°C).

## 2.15 | Total proteome analysis using shotgun proteomics

*K. pneumoniae* were grown on MacConkey agar plates overnight (37°C). A single colony of *K. pneumoniae* was used for inoculation of 2 mL LB media for overnight culture, which was then transferred to 10 mL fresh LB media and further incubated (1 h, 37°C, 160 rpm). Equal numbers of bacteria were grown in LB media in the presence or absence of 1  $\mu\text{g}/\text{mL}$  PB or 20  $\mu\text{g}/\text{mL}$  Gentamicin and additionally 10  $\mu\text{g}/\text{mL}$  *Kp*-ctr OMVs (90 min, 37°C, 160 rpm). Afterwards, equal amounts of bacteria were used for proteomics approach. For that, cells were washed twice in PBS and were resuspended in 300  $\mu\text{L}$  lysis buffer (2% sodium lauroyl sarcosinate (SLS), 100 mM ammonium bicarbonate). Afterwards, cells were incubated at 95°C for 15 min. The

protein concentration was determined by bicinchoninic acid protein assay (Thermo Scientific). Proteins were reduced with 5 mM Tris(2-carboxyethyl) phosphine (Thermo Fischer Scientific) at 90°C for 15 min and alkylated using 10 mM iodoacetamid (Sigma Aldrich) at 25°C for 30 min in the dark. For tryptic digestion 50 µg protein was incubated and 1 µg of trypsin (Serva Electrophoresis GmbH, Heidelberg, Germany) at 30°C overnight in presence of 0.5% SLS. After digestion, SLS was precipitated by adding a final concentration of 1.5% trifluoroacetic acid (TFA, Thermo Fischer Scientific). Peptides were desalted by using C18 solid phase extraction cartridges (Macherey-Nagel, Düren, Germany). Cartridges were prepared by adding acetonitrile (ACN), followed by equilibration with 0.1% TFA. Peptides were loaded on equilibrated cartridges, washed with 5% ACN and 0.1% TFA containing buffer and finally eluted with 50% ACN and 0.1% TFA. Dried peptides were reconstituted in 0.1% TFA and then analyzed using liquid-chromatography-mass spectrometry (MS) carried out on a Exploris 480 instrument connected to an Ultimate 3000 RSLC nano and a nanospray flex ion source (all Thermo Scientific). Peptide separation was performed on a reverse phase HPLC column (75 µm × 42 cm) packed in-house with C18 resin (2.4 µm; Dr Maisch). The following separating gradient was used: 94% solvent A (0.15% formic acid) and 6% solvent B (99.85% ACN, 0.15% formic acid) to 25% solvent B over 66 min, and an additional increase to 35% solvent B over 24 min at a flow rate of 300 nL/min. Peptides were ionized at a spray voltage of 2.3 kV, ion transfer tube temperature set at 275°C, 445.12,003 m/z was used as internal calibrant. MS raw data was acquired on an Exploris 480 (Thermo Scientific) in data independent acquisition mode with a method adopted from (Bekker-Jensen et al., 2020). In short, spray voltage was set to 2.3 kV, funnel RF level at 55, and heated capillary temperature at 275°C. For DIA experiments full MS resolutions were set to 120,000 at m/z 200 and full MS, AGC (Automatic Gain Control) target was 300% with an IT of 50 ms. Mass range was set to 350–1400. AGC target value for fragment spectra was set at 3000%. 45 windows of 14 Da were used with an overlap of 1 Da. Resolution was set to 15,000 and IT to 22 ms. Stepped HCD collision energy of 25, 27.5, 30% was used. MS1 data was acquired in profile, MS2 DIA data in centroid mode.

Analysis of DIA data was performed using DIA-NN version 1.8 (Demichev et al., 2020) using an uniprot protein database from *K. pneumoniae*. Full tryptic digest was allowed with two missed cleavage sites, and oxidized methionines and carbamidomethylated cysteins. Match between runs and remove likely interferences were enabled. The neural network classifier was set to the single-pass mode, and protein inference was based on genes. Quantification strategy was set to any LC (high accuracy). Cross-run normalization was set to RT-dependent. Library generation was set to smart profiling. DIA-NN outputs were further evaluated using the SafeQuant (Ahrné et al., 2013; Glatter et al., 2012) script modified to process DIA-NN outputs.

## 2.16 | Sample preparation lipidomics

A PB-sensitive (*K. pneumoniae*) and -resistant (*KpR*) *K. pneumoniae* strain were treated with 1 µg/mL PB (*K. pneumoniae*) or 64 µg/mL PB (*KpR*), or left untreated as control, grown for 6 h (see bacterial culture and isolation of outer membrane vesicles) and used for lipid isolation. For lipid analysis, OMVs were isolated via ultrafiltration and size exclusion chromatography, then pelletized through ultracentrifugation (2 h, 100,000 × g, 4°C; rotor F50L and tubes: Thermo Fisher Scientific), and equal amounts of bacteria were washed with PBS. For total lipid isolation, OMV and bacterial pellets were resuspended in 150 µL chloroform, 300 µL methanol, and 120 µL H<sub>2</sub>O, and shaken for 10 min (4°C, 1400 rpm) using a thermomixer. Subsequently, 150 µL chloroform and 150 µL 0.85% potassium chloride were added, and the samples were centrifuged (10 min, 4°C, 21,000 × g). The lower phase was used for lipid analysis. For lipid A isolation, the OMV and bacterial pellets were resuspended in 1520 µL of a pre-mixed one-phase Band D mix (1:2:0.8 chloroform:methanol:PBS) and incubated for 20 min with shaking (room temperature (RT), 21,000 × g). The samples were then centrifuged (10 min, RT, 21,000 × g), and the pellets were dissolved in 1520 µL of the pre-mixed one-phase Band D mix, followed by another centrifugation step (10 min, RT, 21,000 × g). The pellets were dissolved in 360 µL of a mild hydrolysis mix (50 mM sodium acetate, 1% SDS, pH 4.5) and incubated for 1 h at 95°C. After cooling down the samples, 400 µL of chloroform, 400 µL of methanol, and 10 µL of an internal lipid standard (LPE 13:0, PE 40:8, PG 40:8, CL 56:4, Cer 22:1;2, HexCer 26:1;2 and SM 24:1;2 each lipid concentration was 1 mg/mL and they were mixed to equal amounts) were added. The samples were mixed by vortexing and then centrifuged (10 min, RT, 21,000 × g). The lower phase was collected in a glass tube. The upper phase of the samples was mixed with 360 µL of the lower phase from the two-phase Band D mix (2:2:1.8 chloroform:methanol:PBS), mixed by vortexing, and centrifuged (10 min, RT, 21,000 × g). The lower phase was collected into the same glass tube as the first lower phase. A defined volume of the mixed lower phases was used for lipid analysis.

## 2.17 | Analysis lipidomics

The relative quantification and annotation of lipids was performed using HRES-LC-MS/MS. The chromatographic separation was performed using a Acquity Premier CSH C18 column (2.1 × 100 mm, 1.7 µm particle size, VanGuard, Waters, Massachusetts, USA), a constant flow rate of 0.3 mL/min with a mobile phase A (10 mM Ammonium Formate in 6:4 ACN:water) and a phase B (9:1 Isopropanol:ACN; Honeywell, Morristown, New Jersey, USA) at 40°C. The injection volume was 5 µL. The mobile phase profile consisted of the following steps and linear gradients: 0–1.5 min constant at 37% B; 1.5–4 min from 37% to 45% B; 4–5 min

from 45% to 52% B; 5–8 min from 52% to 58% B; 8–11 min from 58% to 66% B; 11–14 min from 66% to 70% B; 14–18 min from 70% to 75% B; 18–20 min from 75% to 98% B; 20–25 min constant at 98% B; 25–25.1 min from 98% to 37% B; 25.1–30 min constant at 37% B.

For the measurement, a Thermo Scientific ID-X Orbitrap mass spectrometer was used. Ionisation was performed using a high temperature electro spray ion source at a static spray voltage of 3500 V (positive) and a static spray voltage of 2800 V (negative), sheath gas at 50 (Arb), Auxiliary Gas at 10 (Arb), and Ion transfer tube and Vaporizer at 325°C and 300°C.

For lipid analysis MS measurements, data dependent MS2 measurement were conducted applying an orbitrap mass resolution of 120 000 using quadrupole isolation in a mass range of 200–2000 and combining it with a high energy collision dissociation (HCD). HCD was performed on the ten most abundant ions per scan with a relative collision energy of 25%. Fragments were detected using the orbitrap mass analyser at a predefined mass resolution of 15,000. Dynamic exclusion with and exclusion duration of 5 s after 1 scan with a mass tolerance of 10 ppm was used to increase coverage. For lipid A MS measurement, data dependent MS2 measurement were conducted applying an orbitrap mass resolution of 240,000 using quadrupole isolation in a mass range of 1500–2000 and combining it with a high energy collision dissociation (HCD). HCD was performed on the two most abundant ions per scan with a relative collision energy of 25%. Fragments were detected using the orbitrap mass analyser at a predefined mass resolution of 15,000. Dynamic exclusion with and exclusion duration of 5 s after 1 scan with a mass tolerance of 10 ppm was used to increase coverage.

For lipid data analysis, Compound Discoverer 3.3 (Thermo-Fisher Scientific) was used for lipid annotation by matching accurate mass and MS2 spectra against the MS/MS library MS-DIAL LipidBlast (version 68). For the semi-quantitative comparison of lipid abundance, annotated peaks were integrated using Compound Discoverer 3.3 (Thermo Scientific) and normalization by the default method provided by Compound Discoverer 3.3. The data were normalized to the maximum peak area sum of all samples, the *p*-value per group ratio calculated by a one-way ANOVA with Tukey as post-hoc test, and the *p*-value adjusted using Benjamini–Hochberg correction for the false-discovery rate. The *p*-values were estimated by using the log-10 areas.

For lipid A data analysis, Free Style 1.7 SP2 (Thermo-Fisher Scientific) was used for lipid annotation by manual analysis. For the semi-quantitative comparison of lipid abundance, annotated peaks were integrated using Skyline 22.2.0.255 (MacCoss Lab, Department of Genome Sciences, University of Washington) and normalization by the number of outer membrane vesicles or bacterial OD.

## 2.18 | High performance liquid chromatography (HPLC) and tandem mass spectrometry

Increasing amounts of Polymyxin B (PB; 0–10 µg/mL) were used for incubation of  $2 \times 10^9$  *Kp*-ctr OMVs or *Kp*-PB OMVs (15 min, RT, 1400 rpm) on a thermomixer. Subsequently, the samples were ultracentrifuged (2 h, 100,000 × *g*, 4°C), and the supernatant was transferred into a new reaction tube. OMV pellets were resuspended in PBS (0.1 µm filtered). Both, the supernatant and OMV samples were mixed 1:1 with ACN and used for HPLC, which was carried out on an Agilent 1260 Infinity II system using a reverse phase Agilent ZORBAX Eclipse Plus C18, 2.1 × 50 mm, 1.8 µm. The two mobile phases consisted of water with 0.1% formic acid (solvent A) and ACN with 0.1% formic acid (solvent B). The following gradient was used with a flow rate of 0.3 mL/min: A with 5% B (0–1 min), 95% B (1–25 min), 100% B (25–26 min), 100% B (26–30 min), 5% B (30–31 min), 5% B (31–36 min). Internal standards were eluted with a retention time of 10.4 min. The mass spectrometer, Agilent G470A LC/TQ, was operated in multi reaction monitoring (MRM) mode targeting fragments of 2<sup>+</sup> and 3<sup>+</sup> Polymyxin B (1202.74 amu). The following transitions were used for quantification: 603/241, 603/233, 603/202, 402/233, 402/123 and 402/101 amu. Ionisation was achieved with the following parameters to the Agilent Jet Stream source: sheet gas temperature: 350°C with a flow of 9 L/min, nebulizer pressure 45 psi, capillary voltage 4000 V, nozzle voltage 1000 V. Data recording and evaluation was carried out with the Agilent MassHunter Workstation 10.0.

## 2.19 | Binding and saturation assay of OMVs

*Kp*-ctr OMVs (10 µg/mL) were incubated with or without 3 µg/mL PB or 3 µg/mL PB were incubated for 15 min, RT on a thermomixer (300 × *g*). Samples were afterwards ultracentrifuged for 2 h at 100,000 × *g*, 4°C. The supernatant or the pellet resuspended in LB media were used for *K. pneumoniae* growth. *K. pneumoniae* were grown on MacConkey agar plates overnight (37°C). A single colony of *Klebsiella* was used for inoculation of 2 mL LB media for overnight culture, which was transferred to 10 mL fresh LB media and further incubated (1 h, 37°C, 160 rpm). An optical density of 0.0005 was used to inoculate the supernatant or the pellet fraction from the OMVs. *K. pneumoniae* were grown at 37°C, 160 rpm for 6 h. Afterwards, bacteria were plated on MacConkey agar plates and incubated over night at 37°C to determine colony forming units. Biological replicates were performed in technical duplicates.

## 2.20 | NPN assay

*Kp*-ctr OMVs or *Kp*-PB OMVs ( $1 \times 10^9$  OMVs/well) were incubated with increasing amounts of PB (5–500  $\mu\text{g}$ /well) or 10% Saponin (Carl Roth GmbH & Co KG), 1 mM KCN (Sigma-Aldrich, St. Louis, USA) and 22.5  $\mu\text{M}$  1-N-phenylnaphthylamine (NPN; Sigma-Aldrich) using a black 384-well plate. Fluorescence intensity was directly measured using a microplate reader infinite F200Pro (Tecan, Männedorf, Switzerland; RT, bandwidth: 5 nm, excitation wavelength: 356/350 nm; emission spectra: 410/420 nm, integration time: 20  $\mu\text{s}$ , measurement every 20 s for 20 cycles, mean values of one sample were used for further calculations). Samples without PB were used as blank and subtracted afterwards. The saponin sample was set to 100% and results are shown relative to it.

## 2.21 | Artificial vesicles

The required amount of lipids (see Table S1) was combined in a glass vial and dried under a stream of  $\text{N}_2$  until the lipid cake was completely dry. The dried lipids were rehydrated with 1 mL 0.1  $\mu\text{m}$  filtered PBS for 1 h, with vigorous vortexing in between. Subsequently, samples were extruded using a mini extruder (Avanti Polar Lipids, Inc.) equipped with a 0.1  $\mu\text{m}$  polycarbonate membrane (Avanti Polar Lipids, Inc.). Artificial vesicles were purified through SEC from free lipids, and fractions 6–8 (500  $\mu\text{L}$  each) were pooled and concentrated for further use, following the same procedure as described for OMV purification.

## 2.22 | *Galleria mellonella* infection model

*Galleria mellonella* were purchased from fauna topics (Rielingshausen, Germany) and kept in the dark at 28°C until they reached a weight range between 250 and 350 mg. Food (TropicShop, Nordhorn, Germany) was changed twice a week. Larvae were infected in groups of 10–15 animals through the last proleg pair intra-hemocoelically using a manual microsyringe pump (World Precision Instruments, Sarasota, USA), needle (B. Braun, Melsungen, Germany, 0.45 mm  $\times$  10 mm) and syringe (Becton, Dickinson and Company, Franklin Lakes, USA). For infection experiments, *K. pneumoniae* were grown on MacConkey agar plates overnight (37°C). A single colony of *K. pneumoniae* was used for inoculation of 2 mL LB media for overnight culture, which was then transferred to 10 mL fresh LB media and further incubated (1 h, 37°C, 160 rpm). Bacteria were harvested by centrifugation and resuspended in sterile PBS. For injection, 10  $\mu\text{L}$  PBS as a control or *K. pneumoniae* suspension (66,666 CFU/larvae) with or without *Kp*-ctr OMVs ( $5 \times 10^{10}$  OMVs/larvae) or artificial vesicles containing 40% KLA ( $1 \times 10^{10}$  vesicles/larvae) mixed or not mixed with Polymyxin B (1  $\mu\text{g}$  PB/larvae) were used. The larvae were incubated at 37°C with food and scored each 24 h for 7 days post infection. Larvae that were not responsive to touch were scored as dead.

## 2.23 | Ethical statement

Experiments with human lung tissue slices were approved by the ethics committee of the Hannover Medical School (MHH, Hannover, Germany, no. 8867\_BO\_K\_2020 and no. 2923-2015) and are in compliance with *The Code of Ethics of the World Medical Association* (number 2701–2015). All patients or their next of kin gave written informed consent for the use of lung tissue for research.

## 2.24 | Statistics

Data are shown as mean values  $\pm$  SEM for at least three biologically independent experiments. Prism 10.0.2 (GraphPad, La Jolla, USA) was used. The one-way ANOVA (Tukey's multiple comparisons test) or two-way ANOVA (Sidak's multiple comparisons test) tests or *t*-tests were performed for unpaired samples. *p*-values  $\leq 0.05$  were considered statistically significant. If not indicated otherwise, tests were performed versus corresponding control (\*).

# 3 | RESULTS

## 3.1 | Stress conditions alter the amount and size of *K. pneumoniae* OMVs

To test the impact of a range of stress conditions on vesiculation of *Klebsiella pneumoniae* (*K. pneumoniae*; *Kp*), bacteria were cultured under different experimental conditions. *K. pneumoniae* was subjected to the following stress conditions: LB media with pH 5 or pH 9, temperatures of 20°C or 40°C, treatment with sub-inhibitory concentrations of Gentamicin, Polymyxin B (PB),

or H<sub>2</sub>O<sub>2</sub>, and incubation in NaCl or H<sub>2</sub>O for 90 minutes. For control, *K. pneumoniae* was cultured in LB media. Quantification of released vesicles was achieved by nano-flow cytometry (nFCM). While most of the stress conditions resulted in a moderate increase in vesiculation (Figure 1a), PB led to the formation of significantly more and smaller vesicles (Figure 1a,b). Furthermore, the use of increasing concentrations of PB demonstrated a dose-dependent increase in vesiculation (Figure 1c), without causing bacterial toxicity at the given concentrations and time point (Figure 1d). To determine whether the clinically used antibiotic Colistin, which has a similar mode of action as PB, also influences vesicle size and quantity, *K. pneumoniae* was stressed with this antibiotic as well. Indeed, Colistin led to a significant increase in vesiculation (Figure S1a) and moreover to significantly smaller vesicles (Figure S1b), comparable to PB stress.

### 3.2 | OMVs mediate protection of *K. pneumoniae* against polymyxins

To investigate the influence of bacterial vesicles on the bacterial response to antibiotics, OMVs from *K. pneumoniae* were isolated using ultrafiltration combined with ultracentrifugation or size exclusion chromatography (SEC). Two types of OMVs were obtained: *Kp*-ctr OMVs (untreated *K. pneumoniae*), and *Kp*-PB OMVs (*K. pneumoniae* stressed with 1 µg/mL PB) after 6 h of cultivation. For the antibiotic-stress induced OMVs, 1 µg/mL PB, a sub-inhibitory concentration was used (Figure S2a). The previously observed increase in OMV release after 90 min of PB stress (Figure 1a) was also present in large scale bacterial cultivation and longer incubation for OMV preparation (Figure S2b). In both isolated vesicle types, the presence of intact bacterial vesicles was visualized via transmission electron microscopy (TEM, Figure S2c). Furthermore, an increased proportion of smaller vesicles and a reduced proportion of larger vesicles was observed in *Kp*-PB OMVs compared to *Kp*-ctr OMVs (Figure S2d). For growth kinetic experiments, *K. pneumoniae* was cultured in the presence of 4 µg/mL PB, and either *Kp*-ctr or *Kp*-PB OMVs, or no OMVs, were added. To reflect the observed elevated vesicle release due to PB stress (Figure 1a and S2b) in the following experiments, OMVs were applied based on the amount of extracellular proteins associated with OMVs to account for an increased dose of OMVs for PB OMVs in comparison to ctr OMVs. The OMV-associated protein concentration was similar for both types of vesicle preparations (Figure S2e). Bacterial growth kinetics showed that 4 µg/mL PB inhibited *K. pneumoniae* growth, while *Kp*-ctr OMVs provided partial protection and allowed bacterial replication in the presence of the antibiotic. In contrast, *Kp*-PB OMVs offered full protection against 4 µg/mL PB and bacterial growth was comparable to untreated control *Klebsiella* (Figure 2a). Yet, the degree of protection depended on the OMV dose (Figure 2b). To test if this also applies to other antibiotics, Colistin, Gentamicin, and Meropenem were used. Colistin, as well as PB, binds LPS, leading to pore formation and cell lysis (Ayoub Moubareck, 2020). Gentamicin and Meropenem exhibit their effect intracellularly: Gentamicin inhibits the protein biosynthesis by binding to the 30S ribosomal subunit; Meropenem inhibits peptidoglycan synthesis. *Kp*-ctr OMVs and *Kp*-PB OMVs protected *K. pneumoniae* from Colistin (Figure 2c): *Kp*-PB OMVs demonstrated a tenfold increase in Colistin protection, *Kp*-ctr OMVs increased it approximately threefold. Even though Gentamicin also increased bacterial vesiculation, none of the tested vesicle types provided protection against Gentamicin as shown by bacterial replication being not altered by the addition of vesicles to the antibiotic in comparison to the antibiotic alone (Figure 2d). It was also tested whether OMVs needed to be induced by the same antibiotic to provide protection. The potential of Gentamicin stress-induced OMVs was tested in the presence of Gentamicin, but these *Kp*-genta OMVs were also not able to confer protection (Figure S3a). Interestingly, both *Kp*-ctr OMVs and *Kp*-PB OMVs partially protected *K. pneumoniae* from Meropenem, as the addition of vesicles enabled stronger bacterial replication than in the antibiotic-only group (Figure 2e). As all the antibiotics tested have different mechanisms of action and target different structures in or on the bacterial cell, these findings suggest that the effectiveness of OMVs in protecting against antibiotics depends on the specific antibiotic's mode of action and only works for antibiotics that interact with the bacterial cell surface.

### 3.3 | OMVs alter protein profile of PB-stressed *K. pneumoniae*

To comprehensively examine the distinct responses to PB and Gentamicin in the presence of OMVs, the protein profile of *K. pneumoniae* subjected to antibiotic stress, with or without *Kp*-ctr OMV treatment, was assessed (Figure 3). Analysis of the proteomic data revealed a varying induction pattern of proteins in response to these antibiotics (Figure 3a,b). Moreover, OMVs were found to restore the stress-induced alterations in *K. pneumoniae* caused by PB, effectively restoring control conditions. However, this was not observed with Gentamicin, where the bacterial protein profile in Gentamicin-stressed bacteria closely resembled that of Gentamicin-stressed bacteria supplemented with OMVs. PB treatment resulted in a notable increase in both significantly up- and down-regulated proteins. The addition of *Kp*-ctr OMVs substantially mitigated this effect, nearly abolishing the alterations in protein expression (Figure 3c). Conversely, this was not evident with Gentamicin treatment, as the OMVs did not alleviate the stress response, consistent with the growth kinetics data (Figure 2d). In-depth analysis of the significantly regulated proteins in PB-treated *K. pneumoniae* revealed an enrichment in proteins associated with the antibiotic response, lipid A and LPS biosynthetic processes, as well as (outer) membrane and integral components of the plasma membrane. However, this observation differed from PB-treated *K. pneumoniae* supplemented with OMVs (Figure 3d). These findings underscore the

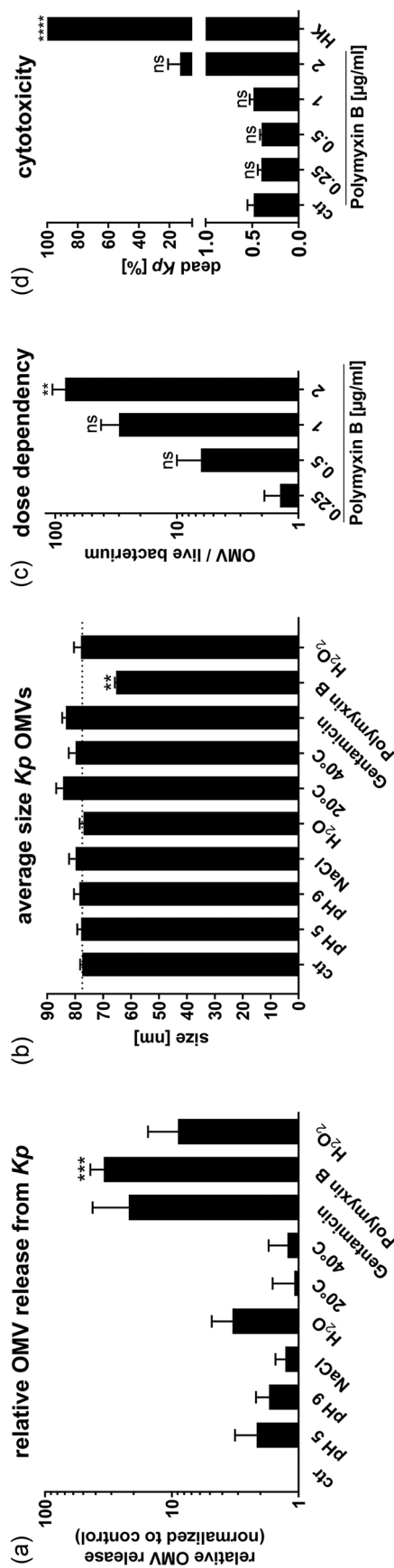


**FIGURE 1** Stress conditions alter the size and quantity of *Klebsiella pneumoniae* (*Kp*) outer membrane vesicles (OMVs). (a–d) *K. pneumoniae* was subjected to the indicated stress conditions or left untreated as a control for 90 min. Bacterial quantification was performed by plating *K. pneumoniae* on agar plates, while the size and amount of released OMVs in the sterile-filtered supernatant. (a) OMV release was calculated relative to the amount of *K. pneumoniae* and normalized to the untreated control (ctr). (b) Average size of OMVs released by stressed and control *K. pneumoniae*. (c) *K. pneumoniae* was incubated with increasing doses of Polymyxin B (PB). OMV release was calculated relative to the quantified *K. pneumoniae* after 90 min of PB treatment (c), and cytotoxicity was assessed by propidium iodide staining (d). The percentage of dead *K. pneumoniae* was calculated relative to heat-killed (HK) bacteria. Bars show mean values ±SEM of three to five independent experiments. Statistics: one-way ANOVA (Tukey's multiple comparisons test); \*\* $p < 0.01$ , \*\*\* $p < 0.001$ , \*\*\*\* $p < 0.0001$  (a, b, d) compared to control (ctr) or (c) to 0.25 µg/mL PB; ns: not significant, ctr: control,  $n \geq 3$ .

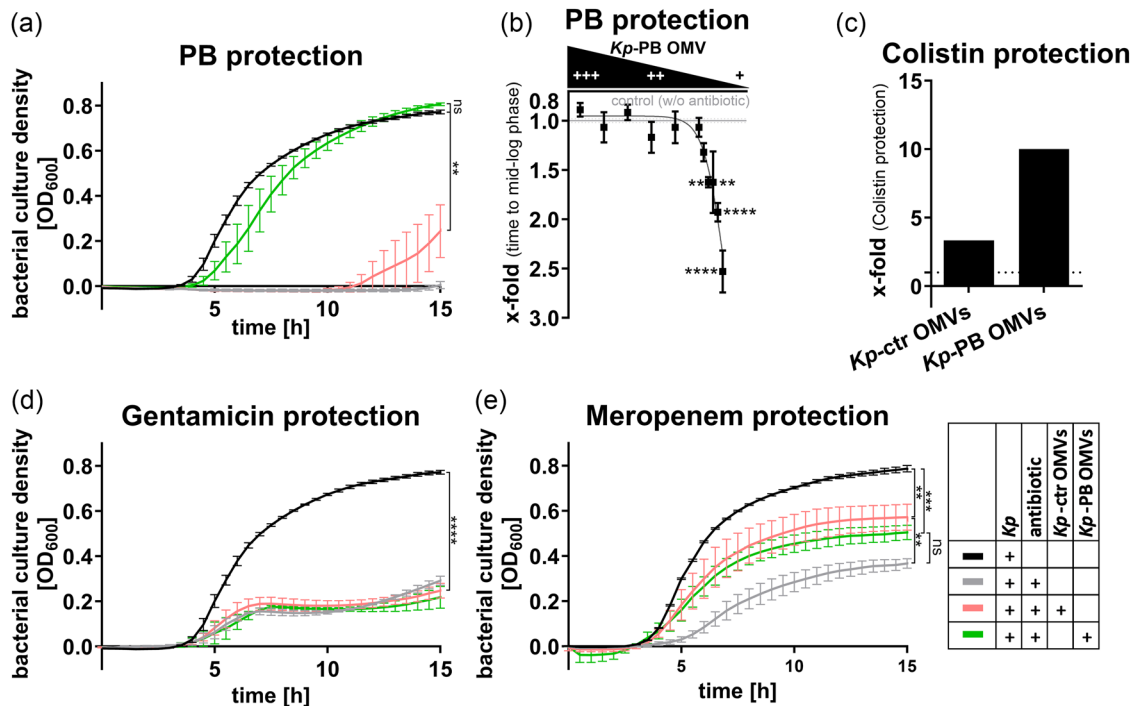


**FIGURE 2** OMVs mediate protection against Polymyxin B (PB) and Colistin. *K. pneumoniae* growth kinetics were determined under continuous shaking at 37°C, and the optical density at 600 nm wave length ( $OD_{600}$ ) was measured every 30 min using a plate reader. All biological replicates were performed in technical triplicates. (a) *K. pneumoniae* was incubated with 4  $\mu\text{g}/\text{mL}$  PB with or without the addition of OMVs from control *K. pneumoniae* (*Kp*-ctr OMVs) or *K. pneumoniae* stressed with 1  $\mu\text{g}/\text{mL}$  PB (*Kp*-PB OMVs) or left untreated as a control. (b) The OMV dose-dependent protection effect of *Kp*-PB OMVs against PB is shown. *K. pneumoniae* was incubated with 4  $\mu\text{g}/\text{mL}$  PB and decreasing concentrations of *Kp*-PB OMVs (ranging from 10  $\mu\text{g}/\text{mL}$  to 4  $\mu\text{g}/\text{mL}$  *Kp*-PB OMVs) or left untreated for control. The x-fold increase in time [h] to reach the mid-log phase ( $OD_{600} = 0.4$ ) is presented, calculated by comparing each *Kp*-PB OMV dose with untreated control *K. pneumoniae*. (c) Protection of *K. pneumoniae* against Colistin mediated by *Kp*-ctr OMVs or *Kp*-PB OMVs is shown as an x-fold change normalized to the untreated control *K. pneumoniae*. (d, e) *K. pneumoniae* was incubated with 35  $\mu\text{g}/\text{mL}$  Gentamicin (d) or 50 ng/mL Meropenem (e) and *Kp*-ctr OMVs or *Kp*-PB OMVs. Untreated *Klebsiella* served as control. Graphs (a–e) show mean values  $\pm$  SEM (a, b, d, e) of three to four independent experiments. Statistics: (a, b, d, e) one-way ANOVA (Tukey's multiple comparisons test), compared to control without antibiotic and as indicated by brackets; \* $p < 0.05$ , \*\* $p < 0.01$ , \*\*\* $p < 0.001$ , \*\*\*\* $p < 0.0001$ ; ns: not significant;  $n \geq 3$ .

differential impact of PB and Gentamicin on the bacterial proteome, as well as the modulatory role of OMVs in attenuating these effects.

### 3.4 | OMVs protect from PB across bacterial families

To delve into this phenomenon, an examination was conducted to ascertain whether *Klebsiella* OMVs could provide protection against the bactericidal effects of PB to various bacteria within the *Enterobacteriaceae* family. This encompassed *Escherichia coli* (*Ec*), *Salmonella enterica* (*Sal*), and a MDR clinical *K. pneumoniae* isolate (*Kp*-i). Culturing these bacteria in the presence of PB, along with either *Kp*-ctr or *Kp*-PB OMVs, revealed that both types of vesicles conferred substantial protection against PB for all tested bacteria (Figure 4a). Additionally, *Kp*-ctr OMVs and *Kp*-PB OMVs extended their protective influence against PB to include *Pseudomonas aeruginosa* and *Legionella pneumophila*, belonging to distinct families (Figure 4b). Notably, *P. aeruginosa* exhibited a more robust level of protection compared to *L. pneumophila*. Subsequently, isolated OMVs from *E. coli*, *Salmonella*, and *Kp*-i were added to bacterial cultures in the presence of PB. Remarkably, OMVs from all tested bacteria demonstrated the capacity to shield recipient bacteria from the bactericidal effects of PB. Furthermore, PB stress-induced OMVs from the respective bacteria generally exhibited a more pronounced protective effect compared to control OMVs (Figure 4a). Given the increasing prevalence of antibiotic resistances within the *Enterobacteriaceae* family (World Health Organization, 2017) and the established role of OMVs in facilitating the transfer of antibiotic resistance genes (Johnston et al., 2023), it was explored whether PB-stress induced OMVs were linked to classical antibiotic resistance. A PB-resistant *K. pneumoniae* strain (*KpR*) was generated and sequenced (Figure S3b). The purified control and PB-induced OMVs from *KpR* could not provide complete protection to a polymyxin-sensitive *K. pneumoniae* strain against 4  $\mu\text{g}/\text{mL}$  PB (Figure S3c) similar to the results obtained with *Kp*-ctr OMVs (see Figure 2a).

Altogether, these findings underscored the inter-family protective potential of OMVs, operating independently to classical antibiotic resistance.

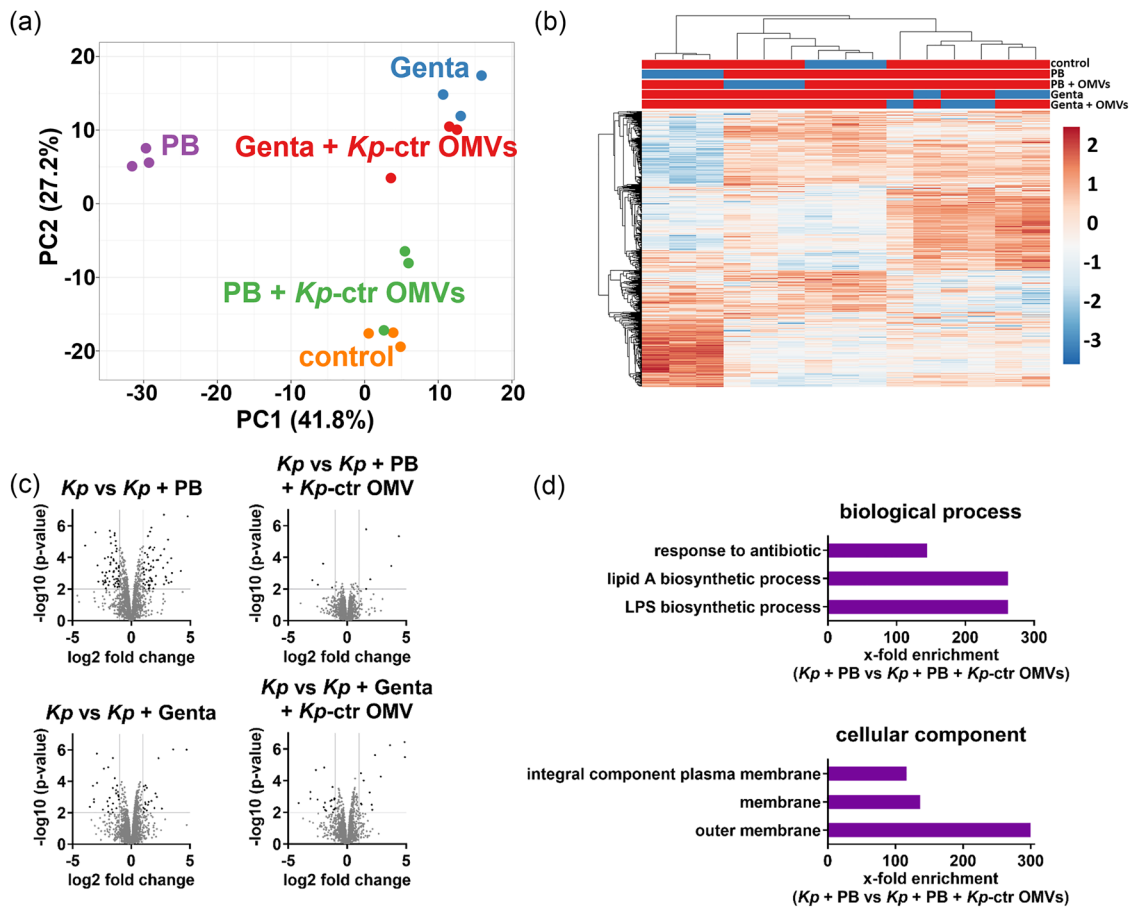


**FIGURE 3** Protein profile of antibiotic-stressed *Klebsiella pneumoniae* was incubated for 90 min with 1  $\mu\text{g}/\text{mL}$  Polymyxin B (PB) or 20  $\mu\text{g}/\text{mL}$  Gentamicin (Genta) with or without *Kp*-ctr OMVs or left untreated as a control. The bacterial protein profile was analyzed by shotgun proteomics and liquid chromatography-mass spectrometry. (a) Principal component analysis of label-free quantitative proteomics data, including all significantly regulated proteins compared to untreated control. (b) Heatmap of all differentially expressed proteins compared to untreated *Klebsiella* is shown for all replicates. Hierarchical clustering was performed. (c) Volcano plots of proteins identified in the differently treated bacteria compared to the untreated control *K. pneumoniae*. The  $\log_2$  fold change (cut-off: 1) versus  $-\log_{10} p$ -value (cut-off: 2) is shown. (d) Gene ontology analysis of the highest enriched pathways in *K. pneumoniae* treated with PB in comparison to *K. pneumoniae* treated with PB in the presence of *Kp*-ctr OMVs is shown. Significantly regulated proteins of both conditions were compared. The top three regulated biological processes (upper) and cellular components (lower) for PB-treated *K. pneumoniae* are shown. Graphs show the results of three biological independent experiments. ctr: control, Genta: Gentamicin, PB: Polymyxin B, PC: principle component.

### 3.5 | OMVs protect *K. pneumoniae* from PB ex vivo and in vivo

To corroborate the OMV-mediated protection against PB and to simulate intricate immune responses occurring in the human lung, precision-cut lung slices (PCLS) were employed in ex vivo infection experiments. These PCLS were infected with *K. pneumoniae*, subjected to PB treatment, and supplemented with *Kp*-PB OMVs, effectively mimicking the infection environment. Bacterial replication was quantified using a colony-forming unit (CFU) assay at 4 and 8 h post-infection (p.i.). Notably, PB treatment substantially reduced CFU counts. However, the additional administration of OMVs restored CFU levels to a range comparable to the control group, consisting solely of *K. pneumoniae* infection (Figure 4c). These results underscore the significance of our findings in the context of complex interactions between bacteria and the host immune system.

Furthermore, this was validated in an in vivo infection model using *Galleria mellonella*. Larvae were infected with *K. pneumoniae* and subsequently subjected to PB treatment alongside the administration of *Kp*-ctr OMVs. Survival rates were monitored over a 7-day period. As the *K. pneumoniae* infection progressed, larval mortality gradually increased, with approximately 70% of larvae dying within a week (Figure 4d). The introduction of PB treatment significantly enhanced survival rates. Strikingly, the combined treatment with PB and *Kp*-ctr OMVs escalated larval mortality rates to 90%. This unveiled the intricate interplay between PB, OMVs, and the host's response in vivo.

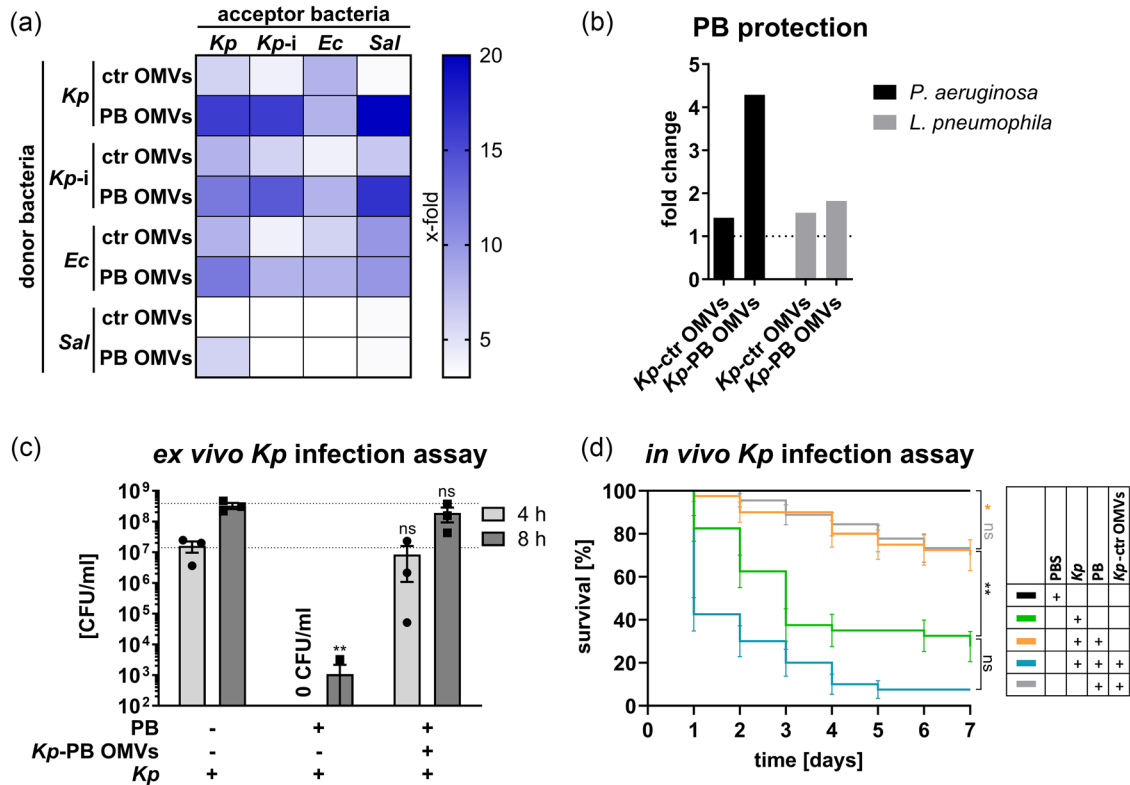


**FIGURE 4** OMVs confer inter-family protection and exhibit ex vivo as well as in vivo protection against PB. (a, b) The protection against PB mediated by OMVs from control or PB-stressed bacteria was determined by performing bacterial growth kinetics. Growth kinetics were determined under continuous shaking at 37°C, and the OD<sub>600</sub> was measured every 30 min using a plate reader. All biological replicates were performed in technical triplicates. The highest concentration of PB that did not significantly alter bacterial growth compared to untreated control bacteria was used to calculate the fold change of Polymyxin B protection, indicating how much more PB the bacteria can tolerate in the presence of the respective OMVs. (a) Heatmap of the protection of different *Enterobacteriaceae* acceptor bacteria against PB in the presence of different *Enterobacteriaceae* OMVs isolated from control (ctr) or PB-stressed donor bacteria. (b) Protection of *Pseudomonas aeruginosa* or *Legionella pneumophila* against PB mediated by *Kp*-PB OMVs or *Kp*-ctr OMVs. (c) Precision-cut lung slices (PCLS) were infected with *K. pneumoniae* for 4 or 8 h, respectively, and additionally treated with 6 µg/mL PB with or without *Kp*-PB OMVs, each in technical duplicates. As a control, PCLS were infected with *K. pneumoniae* without any treatment. Bacterial load at the respective time points is displayed in CFU/mL. (d) *Galleria mellonella* were infected with *K. pneumoniae* by intra-hemocoel injection through the last leg pair and additionally treated with either PB or PB in combination with OMVs. As controls, *G. mellonella* was infected with *K. pneumoniae* or OMVs together with PB. Survival was monitored for 7 days. Per group and replicate, 10–15 larvae were used. Graphs show mean values of 3–5 independent replicates ± SEM (c, d). **Statistics:** (c) two-way ANOVA (Sidak's multiple comparisons test); compared to respective control or (d) unpaired *t*-test; compared as indicated by brackets; \**p* < 0.05, \*\**p* < 0.01; ns: not significant, PB: Polymyxin B, ctr: control; *Kp*: commercially available *Klebsiella pneumoniae* strain (MGH 78578); *Kp*-i: multi-drug resistant *Klebsiella pneumoniae* clinical isolate; *Ec*: *Escherichia coli*; *Sal*: *Salmonella enterica* serovar Typhimurium; *n* ≥ 3.

### 3.6 | OMVs bind PB and can be saturated with PB

PB is known to bind to LPS on the surface of gram-negative bacteria, which is present in large amounts on the surface of OMVs (Ayoub Moubareck, 2020). It was therefore investigated whether the ability of OMVs to bind PB and confer protection to bacteria is mediated by LPS. PB was pre-incubated with or without the addition of OMVs, followed by ultracentrifugation (Figure 5a-i). The resulting supernatant was used for bacterial growth experiments, either with or without fresh PB supplementation (Figure 5b). The replication of *K. pneumoniae* cultured in the supernatant of PB pre-incubation without vesicles was significantly reduced, resembling the CFU levels of *K. pneumoniae* grown in LB media with freshly added PB during bacterial growth (Figure 5b). In contrast, *K. pneumoniae* exhibited normal growth when cultured in the supernatant of pelleted OMVs with PB, a growth pattern similar to *K. pneumoniae*'s behaviour in LB media. These observations strongly indicate the binding of PB by the vesicles, as PB is no longer present in the supernatant but rather present in the pellet. To assess the possibility of vesicle saturation with PB, OMVs were pre-incubated with or without the addition of PB (Figure 5a-ii). After ultracentrifugation, the obtained vesicle pellet was resuspended in LB media for subsequent *K. pneumoniae* growth with fresh PB supplementation (Figure 5c). Notably, *K. pneumoniae*'s replication was significantly hampered when cultured in the resuspended pellet of OMVs with PB with freshly added PB. However, *K. pneumoniae* grew normally when cultured in the resuspended pellet of OMVs that had not been pre-incubated with PB and when PB was freshly added during bacterial growth. These observations suggest that OMVs have a limited PB binding capacity, reaching a state of saturation, rendering them unable to bind additional PB.

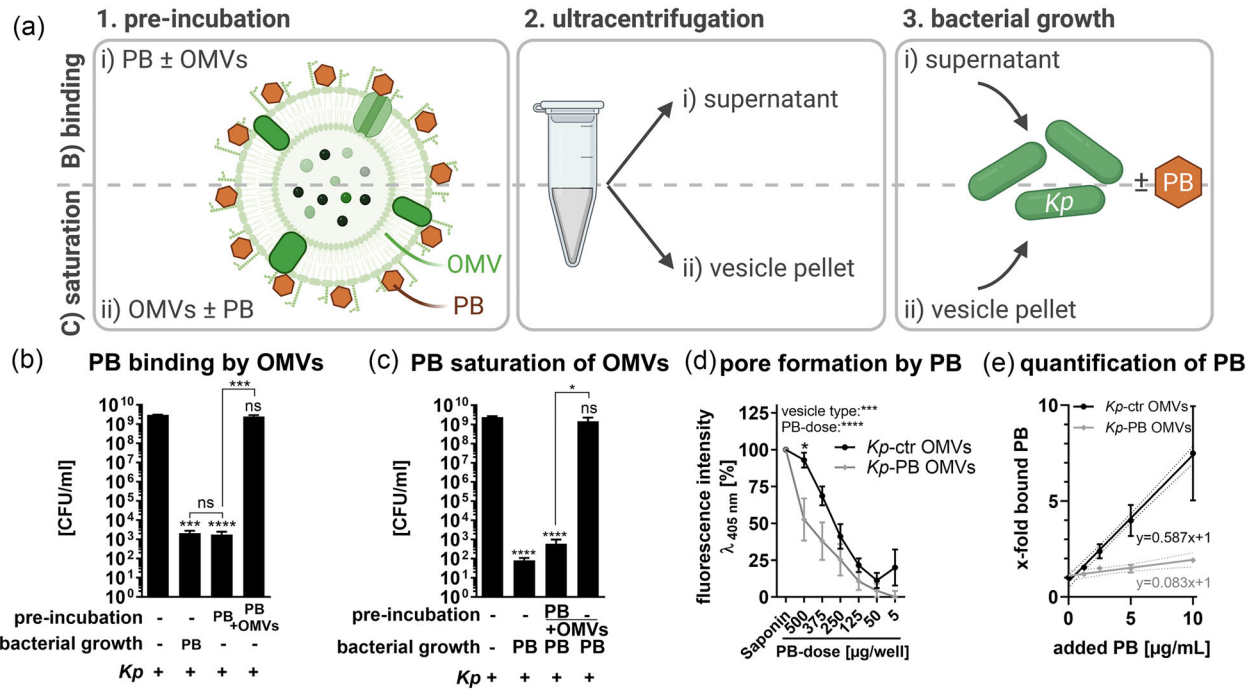


**FIGURE 5** OMVs can bind and become saturated with PB. (a) Schematic illustration (created with biorender.com) of experimental setup used in b and c. (b, c) OMVs were pre-incubated with or without PB and subjected to ultracentrifugation. The vesicle-free supernatant (b) or the OMV-containing pellet (c) was added to *K. pneumoniae* growth experiments with or without the addition of fresh PB while bacterial growth. Bacterial replication was determined by colony forming units (CFU). (d) *Kp*-ctr OMVs or *Kp*-PB OMVs were incubated with increasing amounts of PB (5–500  $\mu\text{g/well}$ ) and 1-N-phenyl-naphthylamine. Fluorescence intensity was measured at 405 nm using a plate reader. Results are shown relative to Saponin, which was used as a positive control for vesicular lysis and is depicted as 100%. (e) *Kp*-ctr OMVs or *Kp*-PB OMVs were incubated with increasing amounts of PB (0–10  $\mu\text{g/mL}$ ). After ultracentrifugation, the bound PB in the vesicle fraction was quantified via mass spectrometry. (b, e) Bars and curves are mean values of three to four independent experiments  $\pm$  SEM. Statistics: (b, c) one-way ANOVA (Tukey's multiple comparisons test) and (d) two-way ANOVA (Sidak's multiple comparisons test), compared to the sample only containing *Kp* or as indicated by brackets (b, c) or Saponin (d); \*  $p < 0.05$ , \*\*\* $p < 0.001$ , \*\*\*\* $p < 0.0001$ ;  $n \geq 3$ .

For validation of PB integration into OMV membranes, PB pre-incubated *Kp*-ctr and *Kp*-PB OMVs were exposed to 1-N-phenyl-naphthylamine (NPN), a molecule that is highly fluorescent in a hydrophobic environment characteristic of the lipid bilayer of OMVs (Figure 5d). During PB-induced pore formation in the OMV membrane, NPN can access the hydrophobic region in the lipid bilayer of OMVs and emit a fluorescent signal. As a positive control for OMV lysis, saponin, a pore-forming agent, was employed. Upon addition of PB to both vesicle types, a dose-dependent increase in fluorescence intensity, indicative of pore formation, was observed. Interestingly, *Kp*-PB OMVs exhibited a lower fluorescence intensity compared to *Kp*-ctr OMVs when exposed to the same dose of PB. This suggests that PB binds less efficiently to *Kp*-PB OMVs than to *Kp*-ctr OMVs, resulting in fewer pores and reduced fluorescence intensity. Moreover, the amount of bound PB in both OMV types was quantified. OMVs were pre-incubated with PB and then subjected to ultracentrifugation, leading to the separation of the vesicle pellet and the soluble PB in the supernatant. The quantification of bound PB was carried out using a triple quadrupole mass spectrometry approach (Figure 5e). Notably, *Kp*-PB OMVs exhibited 1  $\mu\text{g/mL}$  of bound PB from the initial bacterial cultivation under PB stress (Figure S4a). Remarkably, *Kp*-ctr OMVs demonstrated a greater capacity to bind PB compared to *Kp*-PB OMVs, as evidenced by the steeper slope observed in the graph for *Kp*-ctr OMVs (Figure 5e). These results suggest that vesicles can effectively bind PB up to a certain saturation point.

To investigate the protective efficacy of equal amounts of *Kp*-ctr and *Kp*-PB OMVs, both types were utilized in growth kinetic experiments with an equal multiplicity of vesicles per bacterium (Figure S4b). In these experiments, *Kp*-ctr OMVs could fully protect *K. pneumoniae* from PB, whereas *Kp*-PB OMVs provided only partial protection against the antibiotic at the same dose. These experiments underscore that individual *Kp*-ctr OMVs possess a higher capability to protect *K. pneumoniae* from PB compared to individual *Kp*-PB OMVs. These results indicate that the described increased protective ability of *Kp*-PB OMVs against PB (Figures 2 and 4) can be attributed to the heightened vesiculation of *K. pneumoniae* induced by PB treatment (Figures 1a and S2b). Moreover, these findings demonstrate that OMVs can indeed bind and become saturated with PB, leading to the induction of pore formation.

### 3.7 | PB treatment of *K. pneumoniae* alters lipid composition of their released OMVs

To pinpoint the specific OMV component responsible for this phenomenon of antibiotic protection, the potential involvement of several OMV components was tested. As it is known that PB binds to the LPS on the surface of gram-negative bacteria and OMVs have LPS on their surface, we tested the protective capacity of commercial non-vesicular LPS against PB (Ayoub Moubareck, 2020; Schwechheimer & Kuehn 2015). *K. pneumoniae* was grown in the presence of PB and LPS, which yielded only partial protection (Figure S5a), indicating that LPS alone on the OMV surface is not the major protective agent here. Next, the role of vesicular proteins in the PB protection effect was determined. Vesicular proteins were subjected to digestion using Proteinase K, Triton X-100 and Tween-20 (Figure S5b). The protein-digested OMVs retained their ability to protect *K. pneumoniae* from PB, similar to undigested OMVs (Figure S5c), highlighting that the protective effect against PB is not dependent on proteins. Subsequently, the expression of genes typically associated with polymyxin resistance through lipid A structure remodelling of LPS was assessed. Specifically, the expression of *phop*, *phoq* and *pmrK* in PB-treated *K. pneumoniae* and *KpR* and untreated bacterial samples of both strains were examined (Figure S5d). PhoP-PhoQ is a two-component regulatory system, that regulates genes leading to resistance against polymyxins by incorporating 4-aminoarabinose into lipid A, whereby PB cannot properly bind to lipid A anymore (Groisman, 2001). *PmrK* is part of the *pmrHFJKLM* operon, which leads as well to the synthesis of lipid A containing 4-aminoarabinose (Gunn et al., 2000). While the gene expression of all three genes was significantly increased in PB-treated *KpR* samples compared to the respective controls, no significant difference was observed when comparing PB-treated *K. pneumoniae* samples to those without PB. This suggests that none of these three genes is involved in the protective effect mediated by OMVs in polymyxin-sensitive *Klebsiella*.

As no involvement of vesicular LPS and proteins could be detected, the intricacies of the lipid composition within OMVs and their donor bacteria should be elucidated. For that, untargeted lipidomics analysis was conducted on both PB-treated and untreated samples of *K. pneumoniae* and *KpR* strains, as well as their released OMVs (Figure 6). Heatmap and principal component analysis (Figure 6a,b) illustrate the clustering patterns of the lipidomics data. While the lipid composition across the tested bacterial samples appeared relatively similar, distinctive differences emerged in the lipid composition of *Kp*-PB OMVs compared to the other OMV samples. *KpR*-ctr OMVs and *KpR*-PB OMVs clustered closely, sharing similarities with *Kp*-ctr OMVs. The most striking dissimilarities were observed between OMVs derived from PB-treated *K. pneumoniae* and those derived from untreated sensitive *K. pneumoniae*. Several lipids were found to be significantly up- or down-regulated between *Kp*-ctr OMVs and *Kp*-PB OMVs (Figure 6c), resulting in variations in the proportions of different lipid classes (Figure 6d). Given that alterations in lipid A, the innermost region of the LPS, are a common mechanism of polymyxin resistance (Groisman, 2001; Haeili et al., 2017), differences in lipid A patterns between PB-treated and untreated samples of *K. pneumoniae* and *KpR* strains were analyzed. For this purpose, in a targeted approach, the amount of lipid A and possible modifications were determined (Figure 6e,f). The normalized peak area for lipid A was significantly reduced in *Kp*-PB OMVs, indicating a reduction of lipid A amounts, while it was stable in OMVs from *Kp*-ctr, *KpR*-ctr and *KpR*-PB strains (Figure 6e) and in all tested bacterial samples (Figure 6f). The heatmap clearly demonstrates that the normalized peak area of all detectable nominal masses of lipid A was reduced for *Kp*-PB OMVs compared to all other tested OMVs (Figure 6g).

To elucidate the impact of altered lipid composition and lipid A incorporation due to PB-stress on the protective effect of OMVs against the antibiotic, artificial vesicles were generated. These vesicles contained varying amounts of Kdo2-lipid A (KLA; 0%–40%) in addition to lyso-phosphoethanolamine, phosphoethanolamine, phosphoglycerol and sphingomyelin. All artificial vesicles demonstrated a size range comparable to native *Kp*-ctr OMVs (Figure 7a) and were visualized using TEM (Figure 7b). Subsequently, the protection potential of these artificial vesicles was determined. *K. pneumoniae* growth remained unaffected by the addition of artificial vesicles (Figure 7c). Notably, vesicles without KLA were not able to protect *K. pneumoniae* from PB (Figure 7c). However, a dose-dependent protective effect against PB was observed as the concentration of KLA increased within the artificial vesicles (Figure 7d). To confirm this, an ex vivo approach using PCLS was used (Figure 7e). PCLS were infected with *K. pneumoniae* and treated with PB, and additionally, artificial vesicles containing 40% KLA. After 4 h p.i., bacterial load was quantified. PB treatment led to a significantly reduced bacterial load, whereas supplementation with artificial vesicles restored bacterial counts, comparable to the control, which was only infected with *K. pneumoniae*. Furthermore, these data were validated in vivo using *G. mellonella* (Figure 7f). *K. pneumoniae* infection of *Galleria* led to a mortality of approximately 75% over 7 days. PB treatment of the infection significantly enhanced the survival, whereas additional supplementation of artificial vesicles increased the mortality. These results demonstrate that the varying concentrations of lipid A in the native PB stress-induced vesicles determine their protective efficacy against polymyxins.

## 4 | DISCUSSION

Given the alarming rise of multidrug-resistant *Klebsiella* infections, understanding *K. pneumoniae*'s pathogenicity, resistance mechanisms, and potential therapeutic targets is crucial. In this context, OMVs play a key role, facilitating horizontal gene transfer and providing protection against surface-attacking agents, even against last-resort antibiotics like polymyxins (Fulsundar et al.,

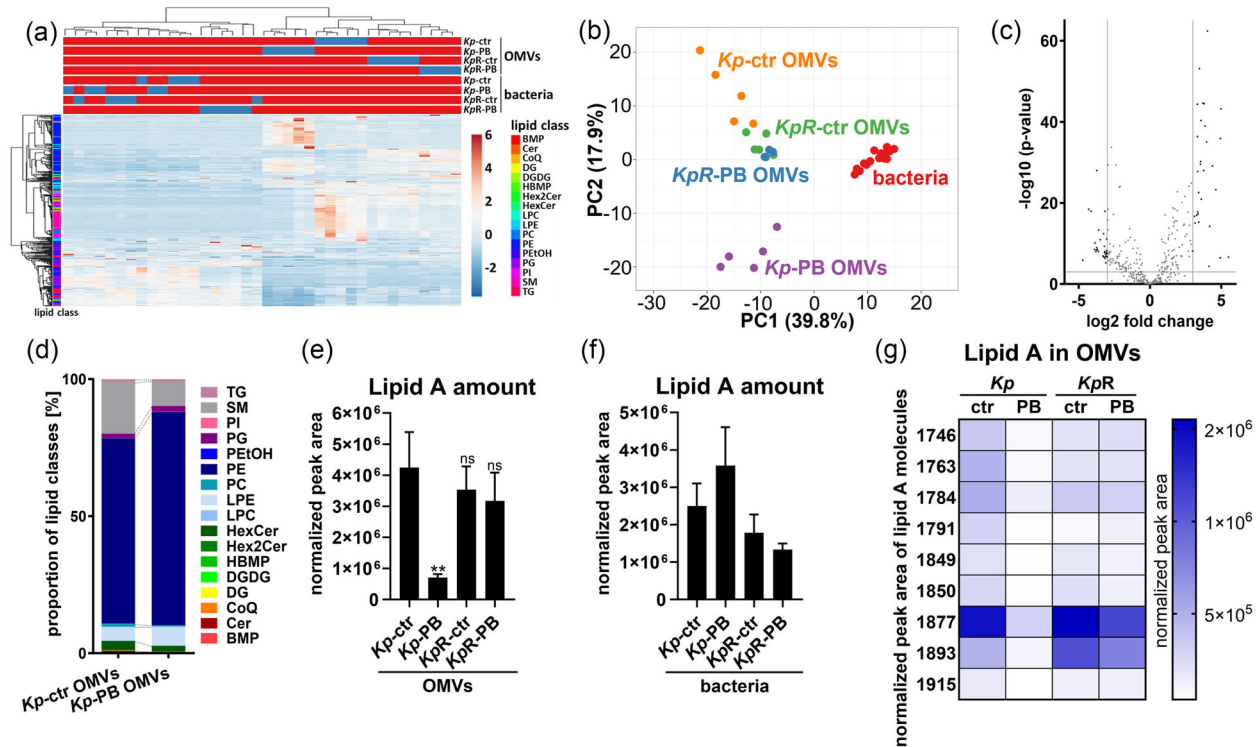


**FIGURE 6** Lipid composition of OMVs and their donor bacteria. (a–g) *K. pneumoniae* (Kp) and PB-resistant *K. pneumoniae* (KpR) were cultured in the presence or absence of PB. OMVs and bacteria were isolated, and their lipids extracted via chloroform/methanol-extraction (a–d) or chloroform/methanol-extraction combined with a mild hydrolysis (e–g) and analyzed via mass spectrometry. (a) Heatmap illustrating the hierarchical clustering of lipid classes across all samples and detected lipids. (b) Principal component analysis of lipidomics data. (c) Volcano plot of up- and down-regulated lipids between Kp-ctr OMVs and Kp-PB OMVs. The  $\log_2$  fold change versus  $-\log_{10}$  p-value is shown. (d) Comparison of lipid class abundancies between Kp-ctr OMVs and Kp-PB OMVs. (e, f) The normalized peak area for lipid A in OMVs (e) or bacterial (f) samples. Lipid A was normalized to the amount of OMVs (e) or the biomass (f) used for lipid extraction. Graphs show the results of four biological independent experiments. (g) Heatmap of the quantification of all detected nominal masses of the m/z ratio of lipid A molecules found in OMV samples. **Statistics:** (e) one-way ANOVA (Tukey's multiple comparisons test) of  $\log_{10}$  transformed data, compared to Kp-ctr OMVs; \*\* $p < 0.01$ ,  $n \geq 3$ ; ns: not significant, TG: Triacylglycerol, SM: Sphingomyelin, PI: Phosphatidylinositol, PG: Phosphatidylglycerol, PEtOH: Phosphatidylethanol, PE: Phosphatidylethanolamine, PC: Phosphatidylcholine, LPE: Lysophosphatidylethanolamine, LPC: Lysophosphatidylcholine, HexCer: Hexosylceramide, Hex2Cer: Dihexosylceramide, HBMP: Hemibismonoacylglycerophosphate, DGDG: Digalactosyldiacylglycerol, DG: Diacylglycerol, CoQ: Coenzyme Q, Cer: Ceramide, BMP: Bismonoacylglycerophosphate.

2014; Kulkarni et al., 2015; Manning & Kuehn, 2011). Until now, it has been unclear whether PB treatment of bacteria impacts the composition of their released OMVs, thereby affecting the protective efficacy of these OMVs against PB. Therefore, this study aimed to investigate how PB treatment impacts OMV composition and, in turn, their protective efficacy against PB.

Here, we report that OMVs protect bacteria from polymyxins in vitro, ex vivo and in vivo by binding PB and acting as decoys. Kp-PB OMVs exhibited a higher protective efficacy than Kp-ctr OMVs due to increased vesiculation under PB stress. However, at the single vesicle level, Kp-PB OMVs showed lower protective efficacy compared to Kp-ctr OMVs. We correlated this reduced single vesicle protective efficacy with a lower amount of lipid A in Kp-PB OMVs, confirmed through artificial vesicles with varying lipid A content. To our knowledge, we are the first to reveal the mechanism behind the altered protective efficacy of Kp-PB OMVs and Kp-ctr OMVs against PB.

Different stress conditions, including Gentamicin, Polymyxin B, and Colistin, alter the size of *K. pneumoniae* OMVs, along with increased vesiculation. Moreover, our findings demonstrate a dose-dependent relationship between PB treatment and the release of OMVs, consistent with previous observations (Fulsundar et al., 2014; Macdonald & Kuehn, 2013; Maestre-Carballa et al., 2019; Yun et al., 2018). To assess the impact of antibiotic stress-induced OMVs from *Klebsiella* on bacterial growth in the presence of antibiotics, Kp-PB OMVs and Kp-ctr OMVs were isolated. Both OMV types protected *K. pneumoniae* from PB in vitro, ex vivo and in vivo as demonstrated in PCLS and *G. mellonella* infection assays. PCLS were used to mimic the complex immune response in the human lung, preserving three-dimensional lung architecture and facilitating physiological interactions among lung cell types, though without immune cell recruitment. *K. pneumoniae* was also protected from PB by OMVs in *G. mellonella* larvae, as previously observed for *A. baumannii* (Park et al., 2021). In vitro, we observed differences in protective capacity between vesicle types. Kp-ctr OMVs partially protected *K. pneumoniae* from 4  $\mu\text{g}/\text{mL}$  PB, while Kp-PB OMVs offered complete protection at this PB dose, enabling normal bacterial replication in the presence of inhibitory PB concentration. Notably, Kp-ctr OMVs appeared to sequester PB molecules down to approximately 2  $\mu\text{g}/\text{mL}$ , whereas cultures supplemented

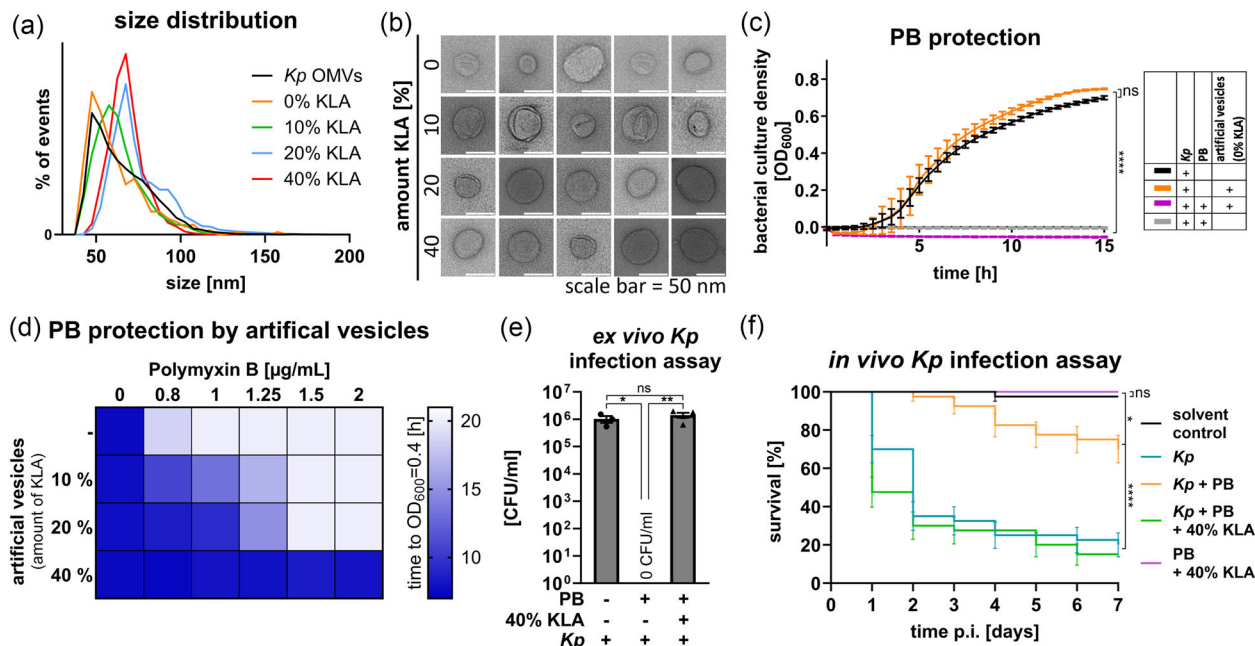


**FIGURE 7** Artificial vesicles containing Kdo2-lipid A protect *K. pneumoniae* from PB. (a–f) Artificial vesicles with increasing amounts of Kdo2-lipid A (KLA, 0%–40%) were generated via membrane extrusion. Size distribution profiles from nFCM (a) and representative TEM images (b) of artificial vesicles are shown. (c, d) The in vitro protection potency of artificial vesicles against PB was determined by performing growth kinetics with *K. pneumoniae*. Growth kinetics were determined under continuous shaking at 37°C, and OD<sub>600</sub> was measured every 30 min using a plate reader. All biological replicates were performed in technical triplicates. (d) A heatmap of the time [h] *K. pneumoniae* need to reach OD<sub>600</sub> = 0.4 (mid of the logarithmic phase) in the presence or absence of increasing amounts of PB (0–2 µg/mL) and with or without artificial vesicles with increasing amounts of KLA (10%–40%) is shown. Graph shows mean values of three independent experiments. (e) Precision-cut lung slices (PCLS) were infected with *K. pneumoniae* for 4 h, and additionally treated with 6 µg/mL PB with or without artificial vesicles containing 40% KLA, each in technical duplicates. As a control, PCLS were infected with *K. pneumoniae* without any treatment. Bacterial load at 4 h post infection is displayed in CFU/mL. Graph shows four biological independent experiments. (f) *Galleria mellonella* were infected with *K. pneumoniae* by intra-hemocoel injection through the last leg pair and additionally treated with either PB or PB in combination with artificial vesicles containing 40% KLA. As controls, *G. mellonella* were injected with PBS (solvent control), *K. pneumoniae* or artificial vesicles together with PB. Survival was monitored for 7 days post-infection (p.i.). Per group and replicate, 10–15 larvae were used. (c–f) Graphs show mean values of three to five independent experiments ± SEM. **Statistics:** (c, e, f) one-way ANOVA (Tukey's multiple comparisons test), compared as indicated by brackets; \**p* < 0.05, \*\**p* < 0.01, \*\*\*\**p* < 0.0001; ns: not significant.

with *Kp*-PB OMVs retained less than 0.5 µg/mL PB (see Figures 2a and S2a for comparison). Previous studies have shown that purified OMVs supplementing bacterial cultures offer protection against various antibiotics, including PB (Kulkarni et al., 2015; Manning & Kuehn, 2011). Furthermore, OMVs demonstrated protective effects across different bacterial families. The ability of *A. baumannii* OMVs to protect bacteria from the human gut microbiota in vitro from PB has previously been demonstrated (Park et al., 2021). These results indicate OMVs' inter-family protective effect against PB by acting as decoys. Furthermore, OMVs were able to protect the fungus *C. albicans* from combined treatment with PB and fluconazole, showcasing the inter-kingdom protective potential of OMVs (Roszkowiak et al., 2019).

Our results align with published data, confirming OMVs' ability to protect *K. pneumoniae* and other bacteria from PB. This study is the first to reveal the altered protective efficacy of OMVs from PB-stressed *K. pneumoniae* compared to OMVs from unstressed *Klebsiella*.

To further understand OMVs' antibiotic protection ability, we tested their effectiveness against antibiotics with diverse modes of action. OMVs provided protection against the polymyxins Colistin and PB, both of which target the gram-negative bacterial cell surface. In contrast, OMVs did not protect against the aminoglycoside Gentamicin, which inhibits protein biosynthesis at the ribosomes. This observation aligns with the inability of OMVs to mitigate Gentamicin stress at the protein level, in contrast to PB stress. Furthermore, OMVs are partially protected against the beta-lactam antibiotic Meropenem, which inhibits bacterial cell wall synthesis. Our findings are consistent with existing literature, showing that *E. coli* OMVs protect against Colistin and Melittin, two membrane-active antibiotics, but not against other antibiotics like Ciprofloxacin, Streptomycin and rimethoprim, each with different modes of action (Kulkarni et al., 2015; Manning & Kuehn, 2011). Altogether, OMVs, by acting as decoys, can only safeguard bacteria from surface-attacking agents, and their effectiveness depends on the mode of action of the antibiotic, which is in contrast to the transport of classical antibiotic resistance genes via OMVs through horizontal gene transfer (Fulsundar et al., 2014).

PB is an amphipathic and cationic agent that binds to the LPS and phospholipids on the surface of bacteria, displacing divalent cations and destabilizing the outer membrane, resulting in pore formation and cell leakage (Ayoub Moubareck, 2020). Given PB's specific mechanism and the presence of LPS on OMVs' surface, we postulated that OMVs may directly bind PB, reducing local antibiotic concentrations and protecting *K. pneumoniae* while reducing bacterial stress, enabling replication in the presence of the antibiotic. To validate our hypothesis, we incubated OMVs with PB, confirming OMVs' ability to bind PB. Yet, there is a limit to PB vesicles can bind, as indicated by saturation in additional PB binding. We quantified this by demonstrating a dose-dependent increase in bound PB on vesicles. Interestingly, *Kp*-ctr OMVs exhibited a higher efficacy in binding PB than *Kp*-PB OMVs, which was independent of the already bound PB we detected in *Kp*-PB OMVs. Previous research indicated OMVs' co-localization with PB using confocal laser scanning microscopy, raising questions about whether incubating OMVs with PB could induce pore formation by the antibiotic (Park et al., 2021). To address this, we incubated OMVs with NPN, a fluorescence-emitting molecule when bound to hydrophobic regions, typically found in the lipid bilayer of OMVs. As the PB dose increased, pore formation increased, as evident by a rise in NPN fluorescence signal emitted by NPN integrated into the vesicular membrane. This underscores PB's mode of action, leading to pore formation in bacterial membranes. Once again, *Kp*-ctr OMVs induced a higher fluorescence intensity than *Kp*-PB OMVs. Based on these findings, we were prompted to assess the individual protective capabilities of both vesicle types at the single vesicle level. We conducted growth kinetic assays using equal numbers of both vesicle types, and the results showed that *Kp*-ctr OMVs exhibited a higher ability to protect *K. pneumoniae* from PB compared to *Kp*-PB OMVs. This suggests a heightened vesicle release in response to PB stress contributes to the previously observed enhanced protection.

To identify the responsible OMV component for the protective effect, we tested various components. Soluble LPS offered only partial protection against PB, indicating that LPS alone is not solely responsible for OMVs' protective effect. We also explored vesicular proteins' involvement but could not establish their contribution. Furthermore, we did not observe the induction of *phoP*, *phoQ* or *pmrK* in the sensitive *K. pneumoniae* strain, but the genes were significantly induced in *KpR*, which was included for comparison. These results suggest that the PhoP-PhoQ regulatory system and the *pmrHFIJKLM* operon, associated with PB resistance, might be the resistance mechanism in the *KpR* strain, but they are not linked to the protective effect of *K. pneumoniae* OMVs against PB. As PB binds to the bacterial surface lipid A, we investigated the OMV lipidome under PB treatment. We analyzed the lipid composition of ctr and PB OMVs from *K. pneumoniae* and *KpR*, as well as their source bacteria, using untargeted lipidomics. PB treatment did not affect the lipid composition of the bacteria, in both *K. pneumoniae* and *KpR*. However, we observed changes in the lipid composition of OMVs, consistent with existing literature (Jasim et al., 2018). *Kp*-PB OMVs significantly differed from *Kp*-ctr OMVs, whereas the lipid profile of *KpR*-PB OMVs and *KpR*-ctr OMVs resembled that of *Kp*-ctr OMVs. In addition to Jasim et al. (Jasim et al., 2018), we demonstrated that PB stress altered the proportion of the lipid classes in the OMVs. Moreover, *Kp*-PB OMVs showed significantly decreased levels of lipid A compared to all other tested OMVs. In line with the changes in the lipidome, specifically in lipid A, it was observed in the proteomics of PB treated *K. pneumoniae* that the corresponding biosynthetic pathways were altered on the protein level.

To investigate the link between decreased lipid A in *Kp*-PB OMVs and their reduced protective effect against PB, we generated artificial vesicles with varying amounts of KLA. These artificial vesicles were introduced into bacterial cultures, demonstrating protective ability against PB depending on the percentage of KLA incorporated. Increasing KLA concentrations in the artificial vesicles improved their ability to bind PB. We further validated these in vitro findings through ex vivo testing with PCLS and in vivo using the *G. mellonella* infection model. Artificial vesicles containing 40% KLA protected *K. pneumoniae* from PB, aligning with data from native *K. pneumoniae* OMVs. These results clearly link the protective feature of OMVs with their lipid A content.

Considering all the obtained data, we propose the following model: The treatment of bacterial infections with last-line antibiotics like polymyxins induces vesiculation in the treated bacteria. These released vesicles exhibit altered lipid composition and reduced lipid A levels compared to ctr OMVs, resulting in weaker polymyxin binding. Nevertheless, the significant increase in vesiculation upon PB treatment allows bacteria to replicate even in otherwise lethal doses of polymyxins, effectively reducing it to sub-lethal levels.

In this study, OMVs were isolated and characterized in accordance with the MISEV 2023 guidelines (Welsh et al., 2024). This approach involved a sequential combination of ultrafiltration, size exclusion chromatography, and ultracentrifugation. Recognizing the potential co-isolation of non-EV contaminants inherent in ultracentrifugation, both methodologies were employed to ensure comprehensive coverage of bacterial EV subpopulations potentially enriched by each method. Vesicle quantification and size distribution profiling were accomplished using nano-flow cytometry. Additionally, the gold-standard of TEM following negative staining was employed to visualize the morphological attributes of the isolated vesicles. Given the absence of established bacterial EV markers in the current guidelines, we followed them accordingly. Furthermore, the potential presence of LPS micelles precluded the utilization of LPS staining as a measure of EV presence. To address this concern, supplementation of the findings with data obtained from in vitro-generated artificial vesicles devoid of potential non-EV contaminants was undertaken. These additional analyses underscored the influence of lipid composition on vesicle-mediated protection across diverse experimental models, ranging from in vitro assays to ex vivo and in vivo settings.

Future studies should compare OMVs released in vivo under PB treatment in terms of quantity and lipid composition with the in vitro stress-induced vesicles. In this study, we used polymyxin doses comparable to the average polymyxin dose of 2  $\mu\text{g}/\text{mL}$ .

in patient serum during Colistin treatment, suggesting that this dose is of physiological relevance in humans (Gontijo & Cavaliere, 2021). Nevertheless, local PB concentrations in the lung may differ from serum levels, warranting further investigation into the local PB dose at the site of infection, particularly in conditions like pneumonia. Unfortunately, obtaining bronchoalveolar lavage fluid (BALF) is challenging and not feasible in severe *Klebsiella* pneumonia cases, and we did not have access to such samples. Furthermore, BALF from severely ill patients receiving various medications may introduce confounding factors, potentially biasing results. In addition, it is essential to meticulously differentiate host- and bacteria-derived EVs.

Our study suggests that the ability of OMVs to protect bacteria from antibiotics depends on the antibiotic's working mechanism. Further analysis is needed to determine if this is a general mechanism against pore-forming antimicrobial peptides acting on the cell surface.

Our findings have significant implications for addressing the growing problem of antibiotic resistance. Understanding how bacteria evade antibiotics, such as through increased vesiculation, underscores the complexity of antibiotic resistance and the need for multifaceted strategies to combat it. The protective effect of OMVs against antibiotics targeting the bacterial cell surface suggests that this mechanism may be a common strategy employed by bacteria to resist such agents. This knowledge is crucial for developing new therapeutic approaches to counter antibiotic-resistant infections, such as designing antimicrobial peptides that do not promote vesiculation.

In conclusion, our study underscores the importance of considering OMVs in antibiotic resistance and their potential to influence bacterial responses to antibiotics. Further research in this field may lead to innovative strategies to counter multidrug-resistant infections and preserve the effectiveness of antibiotics against evolving resistance mechanisms.

## AUTHOR CONTRIBUTIONS

Marie Burt and Anna Lena Jung performed, analyzed, supervised, validated, and visualized experiments. Georgia Angelidou analyzed lipidomics data. Christopher Nils Mais performed mass spectrometry. Christian Preußner quantified vesicles. Timo Glatter performed proteomics experiment. Thomas Heimerl did transmission electron microscopy. Rüdiger Groß and Janis A. Müller contributed to artificial vesicles production and Javier Serrania performed sequencing. Gowtham Boosarpu and Mareike Lehmann contributed mouse PCLS. Danny Jonigk, Lavinia Neubert and Hinrich Freitag provided human lung tissue. Marie Burt, Bernd Schmeck and Anna Lena Jung conceptualized the study. Marie Burt, Nicole Paczia and Anna Lena Jung planned experiments. Marie Burt, Georgia Angelidou, Timo Glatter and Anna Lena Jung prepared figures and analyzed the results. Anna Lena Jung, Bernd Schmeck, Mareike Lehmann, Elke Pogge von Strandmann, Anke Becker and Gert Bange acquired finances. Marie Burt, Bernd Schmeck and Anna Lena Jung wrote the manuscript. All authors have read, discussed and contributed to the manuscript.

## ACKNOWLEDGEMENTS

We thank Dr. Sabrina von Einem for proofreading the manuscript, Lisa Rösser, Mosche Lückhof, Philipp Starck, Laura Pearson and Isabell Beinborn for technical assistance and all lab members for support and discussion. Moreover, we thank PD Dr. Ulrich Matt for providing *Pseudomonas aeruginosa*.

Open access funding enabled and organized by Projekt DEAL.

## CONFLICT OF INTEREST STATEMENT

The authors declare no conflict of interest.

## DATA AVAILABILITY STATEMENT

All data related to the study are available from the corresponding author upon reasonable request.

## ORCID

Janis A. Müller  <https://orcid.org/0000-0002-0347-416X>

Anna Lena Jung  <https://orcid.org/0000-0002-7762-4597>

## REFERENCES

- Ahrné, E., Molzahn, L., Glatter, T., & Schmidt, A. (2013). Critical assessment of proteome-wide label-free absolute abundance estimation strategies. *Proteomics*, 13(17), 2567–2578. <https://doi.org/10.1002/pmic.201300135>
- Arnold, U., & Ulbrich-Hofmann, R. (1999). Quantitative protein precipitation from guanidine hydrochloride-containing solutions by sodium deoxycholate/trichloroacetic acid. *Analytical Biochemistry*, 271(2), 197–199. <https://doi.org/10.1006/abio.1999.4149>
- Ayoub Moubareck, C. (2020). Polymyxins and bacterial membranes: A review of antibacterial activity and mechanisms of resistance. *Membranes*, 10(8), 181. <https://doi.org/10.3390/membranes10080181>
- Bassetti, M., Righi, E., Carnelutti, A., Graziano, E., & Russo, A. (2018). Multidrug-resistant *Klebsiella pneumoniae*: Challenges for treatment, prevention and infection control. *Expert Review of Anti-Infective Therapy*, 16(10), 749–761. <https://doi.org/10.1080/14787210.2018.1522249>

- Bekker-Jensen, D. B., Martínez-Val, A., Steigerwald, S., Rütger, P., Fort, K. L., Arrey, T. N., Harder, A., Makarov, A., & Olsen, J. V. (2020). A compact quadrupole-orbitrap mass spectrometer with FAIMS interface improves proteome coverage in short LC Gradients. *Molecular & Cellular Proteomics: MCP*, 19(4), 716–729. <https://doi.org/10.1074/mcp.TIR119.001906>
- Bhar, S., Edelmann, M. J., & Jones, M. K. (2021). Characterization and proteomic analysis of outer membrane vesicles from a commensal microbe, *Enterobacter cloacae*. *Journal of Proteomics*, 231, 103994. <https://doi.org/10.1016/j.jprot.2020.103994>
- Bierwagen, J., Wiegand, M., Laakmann, K., Danov, O., Limburg, H., Herbel, S. M., Heimerl, T., Dorna, J., Jonigk, D., Preußner, C., Bertrams, W., Braun, A., Sewald, K., Schulte, L. N., Bauer, S., Pogge von Strandmann, E., Böttcher-Friebertshäuser, E., Schmeck, B., & Jung, A. L. (2023). Bacterial vesicles block viral replication in macrophages via TLR4-TRIF-axis. *Cell Communication and Signaling: CCS*, 21(1), 65. <https://doi.org/10.1186/s12964-023-01086-4>
- Bush, L. M., & Vazquez-Pertejo, M. T. (2022). *Klebsiella-, Enterobacter- und Serratia-infektionen*. Hg. v. MSD Manual. Online verfügbar unter <https://www.msmanual.com/de-de/profi/infektionskrankheiten/gramnegative-bakterien/und-infektionen#:~:text=Therapie,-Antibioti-ka%20basierend%20auf&text=Die%20Therapie%20erfolgt%20mit%20Cephalosporinen,sind%2C%20ist%20eine%20Empfindlichkeitstestung%20erforderlich,zuletzt%20gepru%20ft%20am%2021.06.2023>
- Cahill, B. K., Seeley, K. W., Gutel, D., & Ellis, T. N. (2015). *Klebsiella pneumoniae* O antigen loss alters the outer membrane protein composition and the selective packaging of proteins into secreted outer membrane vesicles. *Microbiological Research*, 180, 1–10. <https://doi.org/10.1016/j.micres.2015.06.012>
- Caruana, J. C., & Walper, S. A. (2020). Bacterial membrane vesicles as mediators of microbe—Microbe and microbe—Host community interactions. *Frontiers in Microbiology*, 11, 432. <https://doi.org/10.3389/fmicb.2020.00432>
- Cheng, H. Y., Chen, Y. S., Wu, C. Y., Chang, H. Y., Lai, Y. C., & Peng, H. L. (2010). RmpA regulation of capsular polysaccharide biosynthesis in *Klebsiella pneumoniae* CG43. *Journal of Bacteriology*, 192(12), 3144–3158. <https://doi.org/10.1128/JB.00031-10>
- Ciofalo, O., Beveridge, T. J., Kadurugamuwa, J., Walther-Rasmussen, J., & Høiby, N. (2000). Chromosomal beta-lactamase is packaged into membrane vesicles and secreted from *Pseudomonas aeruginosa*. *The Journal of Antimicrobial Chemotherapy*, 45(1), 9–13. <https://doi.org/10.1093/jac/45.1.9>
- Dell'Annunziata, F., Dell'Aversana, C., Doti, N., Donadio, G., Dal Piaz, F., Izzo, V., De Filippis, A., Galdiero, M., Altucci, L., Boccia, G., Galdiero, M., Folliero, V., & Franci, G. (2021). Outer membrane vesicles derived from *Klebsiella pneumoniae* are a driving force for horizontal gene transfer. *International Journal of Molecular Sciences*, 22(16), 8732. <https://doi.org/10.3390/ijms22168732>
- Demichev, V., Messner, C. B., Vernardis, S. I., Lilley, K. S., & Ralser, M. (2020). DIA-NN: Neural networks and interference correction enable deep proteome coverage in high throughput. *Nature Methods*, 17(1), 41–44. <https://doi.org/10.1038/s41592-019-0638-x>
- Dhital, S., Deo, P., Bharathwaj, M., Horan, K., Nickson, J., Azad, M., Stuart, I., Chow, S. H., Gunasinghe, S. D., Bamert, R., Li, J., Lithgow, T., Howden, B. P., & Naderer, T. (2022). *Neisseria gonorrhoeae*-derived outer membrane vesicles package  $\beta$ -lactamases to promote antibiotic resistance. *microLife*, 3, uqac013. <https://doi.org/10.1093/femsml/uqac013>
- Ellis, T. N., & Kuehn, M. J. (2010). Virulence and immunomodulatory roles of bacterial outer membrane vesicles. *Microbiology and Molecular Biology Reviews: MMBR*, 74(1), 81–94. <https://doi.org/10.1128/MMBR.00031-09>
- Fang, C. T., Chuang, Y. P., Shun, C. T., Chang, S. C., & Wang, J. T. (2004). A novel virulence gene in *Klebsiella pneumoniae* strains causing primary liver abscess and septic metastatic complications. *The Journal of Experimental Medicine*, 199(5), 697–705. <https://doi.org/10.1084/jem.20030857>
- Fulsundar, S., Harms, K., Flaten, G. E., Johnsen, P. J., Chopade, B. A., & Nielsen, K. M. (2014). Gene transfer potential of outer membrane vesicles of *Acinetobacter baylyi* and effects of stress on vesiculation. *Applied and Environmental Microbiology*, 80(11), 3469–3483. <https://doi.org/10.1128/AEM.04248-13>
- Glatter, T., Ludwig, C., Ahrné, E., Aebersold, R., Heck, A. J., & Schmidt, A. (2012). Large-scale quantitative assessment of different in-solution protein digestion protocols reveals superior cleavage efficiency of tandem Lys-C/trypsin proteolysis over trypsin digestion. *Journal of Proteome Research*, 11(11), 5145–5156. <https://doi.org/10.1021/pr300273g>
- Gontijo, A. V. L., & Cavalieri, A. V. G. (2021). Optimal control for colistin dosage selection. *Journal of Pharmacokinetics and Pharmacodynamics*, 48(6), 803–813. <https://doi.org/10.1007/s10928-021-09769-6>
- Groisman, E. A. (2001). The pleiotropic two-component regulatory system PhoP-PhoQ. *Journal of Bacteriology*, 183(6), 1835–1842. <https://doi.org/10.1128/JB.183.6.1835-1842.2001>
- Gunn, J. S., Ryan, S. S., Van Velkinburgh, J. C., Ernst, R. K., & Miller, S. I. (2000). Genetic and functional analysis of a PmrA-PmrB-regulated locus necessary for lipopolysaccharide modification, antimicrobial peptide resistance, and oral virulence of *Salmonella enterica* serovar typhimurium. *Infection and Immunity*, 68(11), 6139–6146. <https://doi.org/10.1128/IAI.68.11.6139-6146.2000>
- Haeili, M., Javani, A., Moradi, J., Jafari, Z., Feizabadi, M. M., & Babaei, E. (2017). MgrB alterations mediate colistin resistance in *Klebsiella pneumoniae* isolates from Iran. *Frontiers in Microbiology*, 8, 2470. <https://doi.org/10.3389/fmicb.2017.02470>
- Hamdi, B., Moussa, I., Berraies, A., Touil, A., Ammar, J., & Hamzaoui, A. (2016). Exacerbations of bronchiectasis: Etiology and outcome. In: 1.5 diffuse parenchymal lung disease. ERS International Congress 2016 abstracts: European Respiratory Society, PA3906.
- Hygienemaßnahmen bei Infektionen oder Besiedlung mit multiresistenten gramnegativen Stäbchen. (2012). Empfehlung der Kommission für Krankenhaushygiene und Infektionsprävention (KRINKO) beim Robert Koch-Institut (RKI). *Bundesgesundheitsblatt, Gesundheitsforschung, Gesundheitsschutz*, 55(10), 1311–1354.
- Jasim, R., Han, M. L., Zhu, Y., Hu, X., Hussein, M. H., Lin, Y. W., Zhou, Q. T., Dong, C. Y. D., Li, J., & Velkov, T. (2018). Lipidomic analysis of the outer membrane vesicles from paired polymyxin-susceptible and -resistant *Klebsiella pneumoniae* clinical isolates. *International Journal of Molecular Sciences*, 19(8), 2356. <https://doi.org/10.3390/ijms19082356>
- Johnston, E. L., Zavan, L., Bitto, N. J., Petrovski, S., Hill, A. F., & Kaparakis-Liaskos, M. (2023). Planktonic and biofilm-derived *Pseudomonas aeruginosa* outer membrane vesicles facilitate horizontal gene transfer of plasmid DNA. *Microbiology Spectrum*, 11(2), e0517922. Advance online publication. <https://doi.org/10.1128/spectrum.05179-22>
- Jung, A. L., Herkt, C. E., Schulz, C., Bolte, K., Seidel, K., Scheller, N., Sittka-Stark, A., Bertrams, W., & Schmeck, B. (2017). *Legionella pneumophila* infection activates bystander cells differentially by bacterial and host cell vesicles. *Scientific Reports*, 7(1), 6301. <https://doi.org/10.1038/s41598-017-06443-1>
- Jung, A. L., Stoiber, C., Herkt, C. E., Schulz, C., Bertrams, W., & Schmeck, B. (2016). *Legionella pneumophila*-derived outer membrane vesicles promote bacterial replication in macrophages. *PLoS Pathogens*, 12(4), e1005592. <https://doi.org/10.1371/journal.ppat.1005592>
- Kim, S. W., Lee, J. S., Park, S. B., Lee, A. R., Jung, J. W., Chun, J. H., Lazarte, J. M. S., Kim, J., Seo, J. S., Kim, J. H., Song, J. W., Ha, M. W., Thompson, K. D., Lee, C. R., Jung, M., & Jung, T. S. (2020). The importance of porins and  $\beta$ -lactamase in outer membrane vesicles on the hydrolysis of  $\beta$ -lactam antibiotics. *International Journal of Molecular Sciences*, 21(8), 2822. <https://doi.org/10.3390/ijms21082822>
- Kulkarni, H. M., Nagaraj, R., & Jagannadham, M. V. (2015). Protective role of *E. coli* outer membrane vesicles against antibiotics. *Microbiological Research*, 181, 1–7. <https://doi.org/10.1016/j.micres.2015.07.008>
- Kulp, A., & Kuehn, M. J. (2010). Biological functions and biogenesis of secreted bacterial outer membrane vesicles. *Annual Review of Microbiology*, 64, 163–184. <https://doi.org/10.1146/annurev.micro.091208.073413>

- Li, J., Nation, R. L., Milne, R. W., Turnidge, J. D., & Coulthard, K. (2005). Evaluation of colistin as an agent against multi-resistant Gram-negative bacteria. *International Journal of Antimicrobial Agents*, 25(1), 11–25. <https://doi.org/10.1016/j.ijantimicag.2004.10.001>
- Li, L., & Huang, H. (2017). Risk factors of mortality in bloodstream infections caused by *Klebsiella pneumoniae*: A single-center retrospective study in China. *Medicine*, 96(35), e7924. <https://doi.org/10.1097/MD.00000000000007924>
- Liu, J., Hsieh, C. L., Gelincik, O., Devolder, B., Sei, S., Zhang, S., Lipkin, S. M., & Chang, Y. F. (2019). Proteomic characterization of outer membrane vesicles from gut mucosa-derived *Fusobacterium nucleatum*. *Journal of Proteomics*, 195, 125–137. <https://doi.org/10.1016/j.jpropt.2018.12.029>
- Liu, Y., Liu, P. P., Wang, L. H., Wei, D. D., Wan, L. G., & Zhang, W. (2017). Capsular polysaccharide types and virulence-related traits of epidemic KPC-producing *Klebsiella pneumoniae* isolates in a Chinese University Hospital. *Microbial Drug Resistance (Larchmont, N.Y.)*, 23(7), 901–907. <https://doi.org/10.1089/mdr.2016.0222>
- Livak, K. J., & Schmittgen, T. D. (2001). Analysis of relative gene expression data using real-time quantitative PCR and the 2(-Delta Delta C(T)) method. *Methods (San Diego, Calif.)*, 25(4), 402–408. <https://doi.org/10.1006/meth.2001.1262>
- Macdonald, I. A., & Kuehn, M. J. (2013). Stress-induced outer membrane vesicle production by *Pseudomonas aeruginosa*. *Journal of Bacteriology*, 195(13), 2971–2981. <https://doi.org/10.1128/JB.02267-12>
- Maestre-Carballa, L., Lluésma Gomez, M., Angla Navarro, A., Garcia-Heredia, I., Martinez-Hernandez, F., & Martinez-Garcia, M. (2019). Insights into the antibiotic resistance dissemination in a wastewater effluent microbiome: Bacteria, viruses and vesicles matter. *Environmental Microbiology*, 21(12), 4582–4596. <https://doi.org/10.1111/1462-2920.14758>
- Manning, A. J., & Kuehn, M. J. (2011). Contribution of bacterial outer membrane vesicles to innate bacterial defense. *BMC Microbiology*, 11, 258. <https://doi.org/10.1186/1471-2180-11-258>
- Mashburn, L. M., & Whiteley, M. (2005). Membrane vesicles traffic signals and facilitate group activities in a prokaryote. *Nature*, 437(7057), 422–425. <https://doi.org/10.1038/nature03925>
- McMillan, H. M., & Kuehn, M. J. (2023). Proteomic profiling reveals distinct bacterial extracellular vesicle subpopulations with possibly unique functionality. *Applied and Environmental Microbiology*, 89(1), e0168622. <https://doi.org/10.1128/aem.01686-22>
- Michalopoulos, A., & Falagas, M. E. (2008). Colistin and polymyxin B in critical care. *Critical Care Clinics*, 24(2), 377–391. <https://doi.org/10.1016/j.ccc.2007.12.003>
- Olaya-Abril, A., Prados-Rosales, R., McConnell, M. J., Martín-Peña, R., González-Reyes, J. A., Jiménez-Munguía, I., Gómez-Gascón, L., Fernández, J., Luque-García, J. L., García-Lidón, C., Estévez, H., Pachón, J., Obando, I., Casadevall, A., Pirofski, L. A., & Rodríguez-Ortega, M. J. (2014). Characterization of protective extracellular membrane-derived vesicles produced by *Streptococcus pneumoniae*. *Journal of Proteomics*, 106, 46–60. <https://doi.org/10.1016/j.jpropt.2014.04.023>
- Paczosa, M. K., & Mecsas, J. (2016). *Klebsiella pneumoniae*: Going on the offense with a strong defense. *Microbiology and Molecular Biology Reviews: MMBR*, 80(3), 629–661. <https://doi.org/10.1128/MMBR.00078-15>
- Park, J., Kim, M., Shin, B., Kang, M., Yang, J., Lee, T. K., & Park, W. (2021). A novel decoy strategy for polymyxin resistance in *Acinetobacter baumannii*. *Elife*, 10, e66988. <https://doi.org/10.7554/eLife.66988>
- Preuß, E. B., Schubert, S., Werlein, C., Stark, H., Braubach, P., Höfer, A., Plucinski, E. K. J., Shah, H. R., Geffers, R., Sewald, K., Braun, A., Jonigk, D. D., & Kühnel, M. P. (2022). The challenge of long-term cultivation of human precision-cut lung slices. *The American Journal of Pathology*, 192(2), 239–253. <https://doi.org/10.1016/j.ajpath.2021.10.020>
- Rafiee, R., Eftekhari, F., & Tabatabaie, S. A. (2017). Extended-spectrum beta-lactamases in cystic fibrosis isolates of *Klebsiella pneumoniae*. *Jundishapur Journal of Microbiology*, 11(1), e61086. <https://doi.org/10.5812/jjm.61086>
- Riwu, K. H. P., Effendi, M. H., Rantam, F. A., Khairullah, A. R., & Widodo, A. (2022). A review: Virulence factors of *Klebsiella pneumoniae* as emerging infection on the food chain. *Veterinary World*, 15(9), 2172–2179. <https://doi.org/10.14202/vetworld.2022.2172-2179>
- Roszkowiak, J., Jajor, P., Guła, G., Gubernator, J., Żak, A., Drulis-Kawa, Z., & Augustyniak, D. (2019). Interspecies outer membrane vesicles (OMVs) modulate the sensitivity of pathogenic bacteria and pathogenic yeasts to cationic peptides and serum complement. *International Journal of Molecular Sciences*, 20(22), 5577. <https://doi.org/10.3390/ijms20225577>
- Russo, T. A., & Marr, C. M. (2019). Hypervirulent *Klebsiella pneumoniae*. *Clinical Microbiology Reviews*, 32(3), e00001–e00019. <https://doi.org/10.1128/CMR.00001-19>
- Schroll, C., Barken, K. B., Krogfelt, K. A., & Struve, C. (2010). Role of type 1 and type 3 fimbriae in *Klebsiella pneumoniae* biofilm formation. *BMC Microbiology*, 10, 179. <https://doi.org/10.1186/1471-2180-10-179>
- Schwechheimer, C., & Kuehn, M. J. (2015). Outer-membrane vesicles from Gram-negative bacteria: Biogenesis and functions. *Nature Reviews Microbiology*, 13(10), 605–619. <https://doi.org/10.1038/nrmicro3525>
- Tran, T. B., Velkov, T., Nation, R. L., Forrest, A., Tsuji, B. T., Bergen, P. J., & Li, J. (2016). Pharmacokinetics/pharmacodynamics of colistin and polymyxin B: Are we there yet? *International Journal of Antimicrobial Agents*, 48(6), 592–597. <https://doi.org/10.1016/j.ijantimicag.2016.09.010>
- Uhl, F. E., Vierkotten, S., Wagner, D. E., Burgstaller, G., Costa, R., Koch, I., Lindner, M., Meiners, S., Eickelberg, O., & Königshoff, M. (2015). Preclinical validation and imaging of Wnt-induced repair in human 3D lung tissue cultures. *The European Respiratory Journal*, 46(4), 1150–1166. <https://doi.org/10.1183/09031936.00183214>
- Welsh, J. A., Goberdhan, D. C. I., O’Driscoll, L., Buzas, E. I., Blenkinsop, C., Bussolati, B., Cai, H., Di Vizio, D., Driedonks, T. A. P., Erdbrügger, U., Falcon-Perez, J. M., Fu, Q. L., Hill, A. F., Lenassi, M., Lim, S. K., Mahoney, M. G., Mohanty, S., Möller, A., Nieuwland, R., ... Witwer, K. W. (2024). Minimal information for studies of extracellular vesicles (MISEV2023): From basic to advanced approaches. *Journal of Extracellular Vesicles*, 13(2), e12404. <https://doi.org/10.1002/jev2.12404>
- World Health Organization. (2017). *WHO publishes list of bacteria for which new antibiotics are urgently needed*. Geneva. Online verfügbar unter <https://www.who.int/news/item/27-02-2017-who-publishes-list-of-bacteria-for-which-new-antibiotics-are-urgently-needed>, zuletzt geprüft am 21.06.2023
- Yun, S. H., Park, E. C., Lee, S. Y., Lee, H., Choi, C. W., Yi, Y. S., Ro, H. J., Lee, J. C., Jun, S., Kim, H. Y., Kim, G. H., & Kim, S. I. (2018). Antibiotic treatment modulates protein components of cytotoxic outer membrane vesicles of multidrug-resistant clinical strain, *Acinetobacter baumannii* DU202. *Clinical Proteomics*, 15, 28. <https://doi.org/10.1186/s12014-018-9204-2>
- Zavan, L., Fang, H., Johnston, E. L., Whitchurch, C., Greening, D. W., Hill, A. F., & Kaparakis-Liaskos, M. (2023). The mechanism of *Pseudomonas aeruginosa* outer membrane vesicle biogenesis determines their protein composition. *Proteomics*, 23(10), e2200464. <https://doi.org/10.1002/pmic.202200464>
- Zhang, X., Qian, C., Tang, M., Zeng, W., Kong, J., Fu, C., Xu, C., Ye, J., & Zhou, T. (2023). Carbapenemase-loaded outer membrane vesicles protect *Pseudomonas aeruginosa* by degrading imipenem and promoting mutation of antimicrobial resistance gene. *Drug Resistance Updates: Reviews and Commentaries in Antimicrobial and Anticancer Chemotherapy*, 68, 100952. <https://doi.org/10.1016/j.drug.2023.100952>

- Zhao, Z., Wang, L., Miao, J., Zhang, Z., Ruan, J., Xu, L., Guo, H., Zhang, M., & Qiao, W. (2022). Regulation of the formation and structure of biofilms by quorum sensing signal molecules packaged in outer membrane vesicles. *The Science of the Total Environment*, 806(Pt 4), 151403. <https://doi.org/10.1016/j.scitotenv.2021.151403>
- Zingl, F. G., Kohl, P., Cakar, F., Leitner, D. R., Mitterer, F., Bonnington, K. E., Rechberger, G. N., Kuehn, M. J., Guan, Z., Reidl, J., & Schild, S. (2020). Outer membrane vesiculation facilitates surface exchange and in vivo adaptation of *Vibrio cholerae*. *Cell Host & Microbe*, 27(2), 225–237.e8. <https://doi.org/10.1016/j.chom.2019.12.002>

## SUPPORTING INFORMATION

Additional supporting information can be found online in the Supporting Information section at the end of this article.

**How to cite this article:** Burt, M., Angelidou, G., Mais, C. N., Preußner, C., Glatter, T., Heimerl, T., Groß, R., Serrania, J., Boosarpu, G., Pogge von Strandmann, E., Müller, J. A., Bange, G., Becker, A., Lehmann, M., Jonigk, D., Neubert, L., Freitag, H., Paczia, N., Schmeck, B., & Jung, A. L. (2024). Lipid A in outer membrane vesicles shields bacteria from polymyxins. *Journal of Extracellular Vesicles*, 13, e12447. <https://doi.org/10.1002/jev2.12447>